INERTIO- AND ELASTO-MAGNETIC FRACTIONATION OF MULTIPLE MICROPARTICLES IN NEWTONIAN AND NON-NEWTONIAN FLUIDS

VIKASH KUMAR

A THESIS SUBMITTED TO

THE FACULTY OF GRADUATE STUDIES

IN PARTIAL FULFILLMENT OF THE REQUIRMENTS

FOR THE DEGREE OF

MASTER OF APPLIED SCIENCE

GRADUATE PROGRAM IN MECHANICAL ENGINEERING

YORK UNIVERSITY

TORONTO, ONTARIO

NOVEMBER 2016

ABSTRACT

Sorting of microparticles and cells using microfluidic platforms has several applications in diagnosis, biotechnology, and medicine. However, the currently available microfluidic sorting techniques have one or more of the following drawbacks such as low throughput, need for diluting sheath flows for operating devices, inability to sort multiple particles simultaneously, low purity and requirement of complicated fabrication methods. In this thesis, a hybrid scheme for sheath-less fractionation of microparticles has been devised by integrating magnetophoresis, inertial focusing and elastic focusing approaches with the concept of pinched flow fractionation. We have taken advantage of inertia, magnetic, drag, and elastic forces to achieve high throughput multiplexed microparticle fractionation. The technique has been tested with respect to parameters such as size of particles, flow rate, device geometry and fluid viscosity (Newtonian vs. non-Newtonian). This sorting method offers a tool to handle heterogeneous samples and can be used for affinity-based immuno-magnetic separation of biological substances.

ACKNOWLEDGEMENTS

I would like to express my sincere gratitude to my supervisor Dr. Pouya Rezai for his continuous support to my Master's research over the last two years. It was an enjoyable journey and fortunately I have had the chance to develop my critical thinking ability, presentation skills and writing skills besides learning how to conduct research professionally. I am grateful to Dr. Rezai for the fact that he not only ably supervised my research but also nurtured me to be an independent researcher on the way. I would have not been able to succeed in this endeavour without his guidance at every stage of my master's research.

I would like to thank Dr. Sunny Leung, my committee member, for his time and support towards my research. I am thankful to Dr. Leung for showing great interest and enthusiasm in improving my research as a committee member. His words of encouragement, invaluable comments and suggestions during the meetings always kept me motivated to perform better.

I am thankful to Dr. Usman T Khan for showing interest in my research and agreeing to serve as a thesis examination member.

I would like to acknowledge the support of all my awesome friends in the ACμTE lab and in the Department of Mechanical Engineering; this journey would not have been same without your support. Thank you all for making these two years a memorable cruise.

TABLE OF CONTENTS

LIST OF FIGURES

GLOSSARY

AR (Aspect ratio) – AR of the channel is defined as ratio of width to height of channel.

CTCs (Circulating tumor cells) - Rare cancer cells found circulating in the blood of humans.

DI (Deionized) water – The water whose ions has been removed and is commonly used in laboratory research.

Drag force - Drag force on an object in a fluid is defined as resistance acting on it due to relative motion of the object with regard to the surrounding moving fluid.

Elastic focusing - The phenomenon of microparticles occupying equilibrium position in the microchannel under the effect of elastic lift forces.

Inertial focusing - The phenomenon of microparticles occupying equilibrium position in the microchannel under the combined effect of shear induced and wall induced lift forces.

ImageJ – It is freeware image processing software developed at National Institutes of Health.

Laminar flow – A type of fluid flow, where fluid particles travel in parallel streamlined layers without any disturbance between the layers.

Magnetophoresis - The phenomenon of movement of magnetic particles under the influence of external magnetic field.

MP (Magnetic particle) - The microsphere having a layer of magnetite and polystyrene onto monodispersed polystyrene core particles.

Multiplex – Handling of multiple analyte or particle at a time is referred to as multiplex process.

NMP (Non-magnetic particle) - The microspheres made from the polystyrene polymer.

Newtonian fluid - Fluids whose viscosity does not change with the rate of shear in the flow.

Non-Newtonian fluid - Fluids whose viscosity changes with the rate of shear in the flow.

PDMS (Polydimethylsiloxane) - One of the most commonly used Siloxane polymer for fabricating microfluidics devices.

PEO (Polyethylene oxide) – PEO is a polymer of monomeric unit Ethylene oxide having chemical formula C_2H_4O. It is mixed in water to make an aqueous solution and was used a substitute for non-Newtonian fluid.

Photolithography – It is microfabrication process which involves transferring a micro-pattern onto a photoresist layer on a Silicon wafer.

Soft lithography – It refers to techniques used for fabricating microfluidics devices, microstructures and micro-patterns using elastomeric materials.

SU-8 photoresist – It is an epoxy based negative photoresist, which gets crosslinked upon exposure to UV (ultraviolet) light.

Sheath flow – The external buffer flow used for operating a device is called sheath flow and it supplied in addition to sample flow in the device.

Chapter One

1 Introduction and Thesis Structure

1.1 Introduction

1.1.1 Background and Motivation

Handling of mixtures of micron-sized entities such as particles and cells in a fluidic sample is of importance in many applications such as diagnostics (e.g. isolation of rare circulating tumor cells and separation of malaria infected red blood cells), biotechnology (e.g. selection of high protein producing cells from a mixture of protein-secreting cells) and environmental assessments (e.g. detection of pathogenic microorganisms in water). There are various techniques available for performing these sorting operations on macroscale such as centrifugation [1], chromatography [2] and filtration [3]. Centrifugation method requires bulky equipment for separation [1]. Achieving high chromatographic separation resolution needs expensive instruments and reagents as well as long operation time [2]. Filtration based methods are often inefficient in performing separation on large-volume or complex samples owing to clogging of filter pores [3].

Microfluidic devices provide a unique platform for achieving separation at microscale with numerous distinct advantages such as lesser reagent requirements, lower operational cost, miniaturized size, portability and filter-less sorting [4–6]. In the literature, several successful attempts have been reported to devise a microfluidic sorting device. These techniques are classified as either active methods, which require an external energy to operate, or passive methods which do not require any external energy. Main active methods are magnetophoretic [7], dielectrophoretic (DEP) [8], optical [9] and acoustic [10] sorting. The passive methods

include pinched flow fraction (PFF) [11], hydrodynamic filtration (HDF) [3], inertial sorting [12], and deterministic lateral displacement (DLD) [13].

1.1.2 Active Microfluidic Sorting Methods

Here, we discuss the active microfluidic sorting techniques reported in the literature. Magnetophoresis refers to movement of magnetic particles (MPs) under the influence of external magnetic field. It has been implemented in microfluidic devices using a permanent magnet or an electromagnet to generate high gradient magnetic fields at desired locations in the device [14,15]. Magnetophoresis has been used for isolating rare circulating tumor cells (CTCs) and separating pathogens from water [16,17]. The target substances to be separated can either be innately magnetic or conjugated with MPs so that their motion can be influenced by the magnetic forces. The separation is achieved based on the difference in force experienced by the particles of different sizes or magnetic content as shown in Fig. 1(a). However the operation of this method requires a sheath flow for pre-focusing of all particles into a single stream [14,18,19]. The throughput of magnetophoretic separation is in the range of ~10^3-10^7 particles per hour [14,18] and the process of fabricating these devices is complicated because it is challenging to embed elements such as magnetic stripes or needles into small microfluidic channels [18].

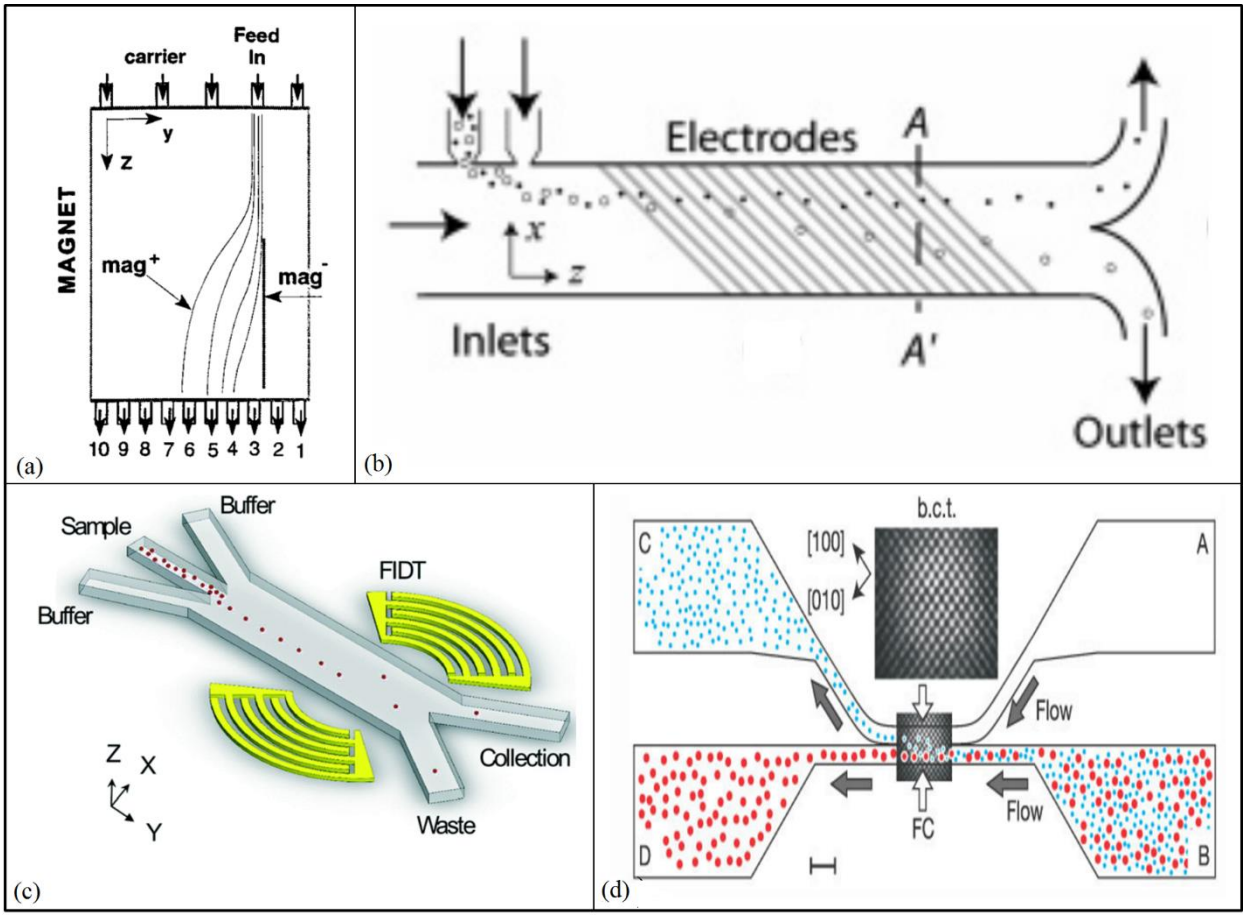

Figure 1. *Active microfluidic particle and cell soritng methods. (a) Magnetic sorting device devised by Chalmers et al.* [19]. *A magnet was positioned by the side of device to attract magnetically tagged objects and separate them from non-magnetic objects. (b) Dielectrophoretic size based particle sorter reported by Kralj et al.* [20]. *Particles were separated using microfabricated electrodes to apply dielectrophoresis force and collected at outlets. (c) Microfluidic acoustic sorter reported by Ren et al.* [21]. *FIDTs (focused interdigital transducers) help in directing the target particles into the collection outlet. (d) Optical fractionation of particles reported by MacDonald et al. [9]. Chamber A contains sheath flow which is used to hydrodynamically focus the particles injected from chamber B and the laser bean is used to deflect the target particles into chamber C while non-target particles are collected into chamber D. All permissions have been obtained for reprinting from the respective publishers.*

The dielectrophoresis (DEP) technique is based on the idea that dielectric particles experience a force when exposed to a non-uniform electric field. For this, microelectrodes are fabricated to generate electric field which exerts force on target particles to separate them from non-target

particles as shown in Fig. 1(b). The magnitude of forces acting on the particles is dependent on several factors such as suspending medium, particles characteristics and frequency of the applied electric field [22,23]. The DEP technique has been used for separating cancer cells from blood and sorting multiple bacterial targets simultaneously [24,25]. The major limitation of DEP is that it cannot be operated at high flow rates as particles cannot be deflected significantly at high velocities. Fiedler et al. [8] demonstrated sorting at a maximum linear velocity of up to 10 mm s^{-1}.

Acoustic sorting utilizes the forces exerted by bulk or surface acoustic waves on the particles suspended in the fluid to separate or align them as shown in Fig. 1(c). Acoustic sorting methods have been used for separating CTCs from blood and viable mammalian cells from a mixture of viable and non-viable cells [26,27]. The throughput of acoustic based methods is in the order of 10^7 particles per hour while fabrication of acoustic sorting devices is relatively complex.

Optical sorting of particles is based on the fact that particles experience a lateral force when exposed to a focused light source such as a laser beam as shown in Fig. 1(d). Optical fractionation scheme has been used for sorting mitochondria and mammalian cells on microfluidic platform [28,29]. These optical manipulation techniques however require a sheath flow for operation while sorting of more than two particles is yet to be achieved using this method [9,30].

1.1.3 Passive Microfluidic Sorting Methods

The majority of the passive microfluidic sorting techniques which are shown in Fig. 2 work based on the principle of fluid-particle interactions and experiencing forces such as inertia and hydrodynamic forces. In the PFF method, particles are aligned against a wall using a sheath flow on distinct streamlines based on their size and separation is achieved as they are allowed to enter

into an expansion region as shown in Fig. 2(a). PFF has been used to separate cancer cells from white blood cells, to detect single nucleotide polymorphisms, and to sort multiple droplets and bubbles [31–34]. This method requires a sheath flow as much as 10-30 times the sample flow rate for its operation and also works at a low throughput of 10^5-10^6 particles per hour [11,35].

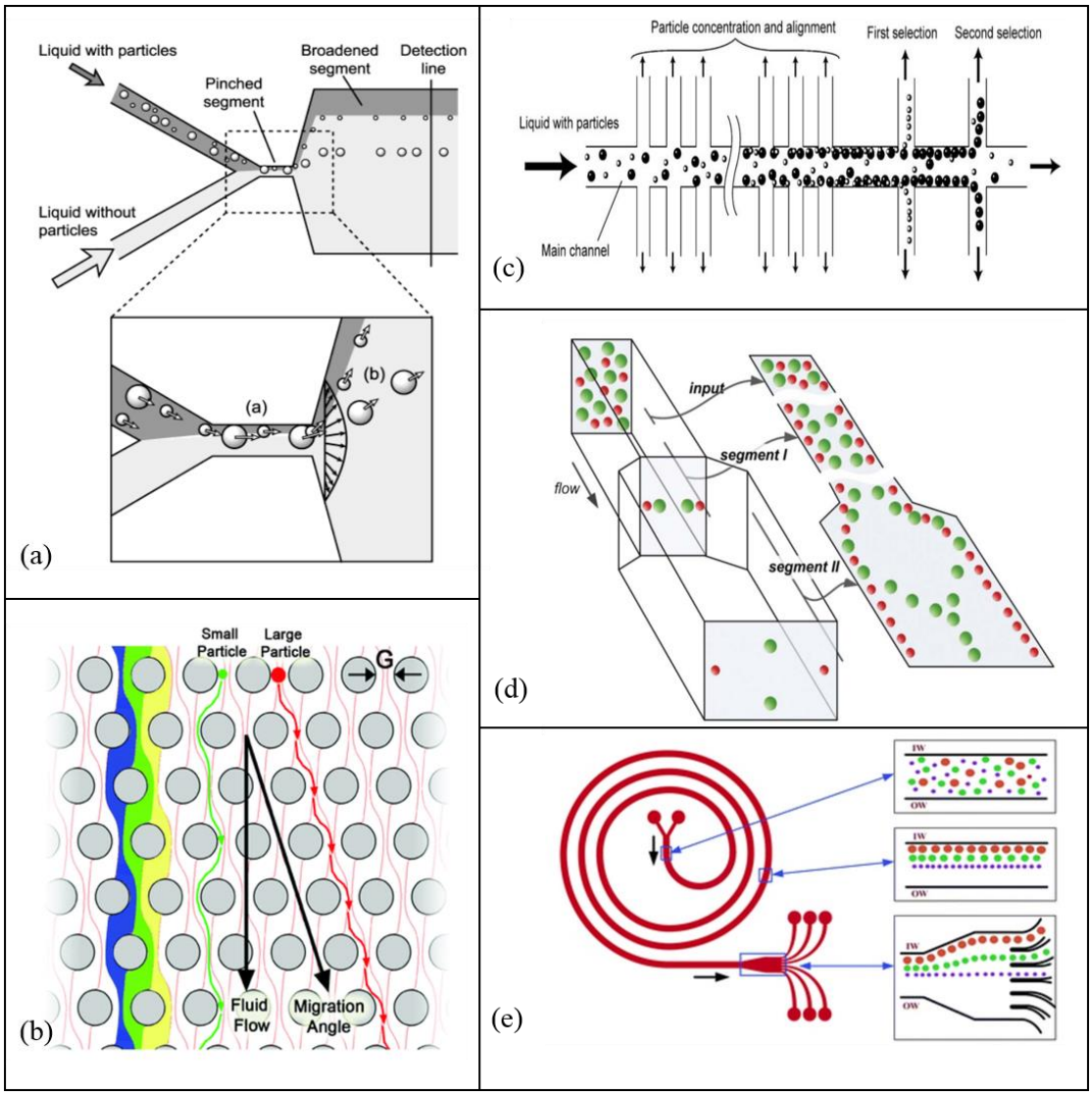

Figure 2. *Passive microfluidic particle and cell sorting methods. (a) Pinch Flow Fractionantion (PFF) method where a sheath flow is used to focus the particles against the wall of a narrow channel in the pinched segment. The focused particles follow different streamlines owing to their different sizes and hence get separated as they enter into a broadened segment [11]. (b) Deterministic Lateral Displacement (DLD) separation method. Particles are fractionated based on their size as micropillars define a cutoff size for the particles, such that particles larger than cutoff would get displaced and move to next lane,*

however particles smaller than cutoff keep following the same lane [36]. *(c) Hydrodynamic Filtration (HDF) technique. A mixture of particles are injected into the device and fluid is drained through side outlets so as to allow particles to get aligned along the walls. Aligned particles are collected into side outlets based on their size as the width of side outlets determines the size of particles that can pass through* [37]. *(d) Inertial sorting of particles in a straight microchannel. Firstly the mixture of particles are focused along the side walls in segment I and are further allowed to enter into segment II where the larger particles get separated and focused inertially in center* [38].*(e) Spiral microfluidic device used for sorting microparticles. Particles are separated using hydrodynamic forces (Dean and inertial forces) generated in curved channels* [39]. *All permissions have been obtained for reprinting from the respective publishers.*

The DLD method performs size based separation of particles using numerous micro-fabricated pillars as shown in Fig. 2(b). DLD has been efficiently used for isolating cancer cells and separating parasites from human blood [40,41] and a comprehensive review of DLD method can be found in McGrath et al. [42]. This method can separate multiple particles simultaneously, however, the fabrication process of micropillars is challenging and operation of the devices is also marred by frequent clogging.

The HDF method allows suspended particles to be aligned against the wall of a channel by draining fluid through its side outlets. Particles are sorted based on their size by controlling the width of these side outlets as shown in Fig. 2(c). HDF has been demonstrated to achieve leukocyte separation from blood and sorting of human lymphocyte cells [37,43]. However, side outlets in HDF devices are prone to clogging when dealing with concentrated mixtures of multiple substances and moreover, it requires a large number of side outlets (50-100) making the operation of the device a challenging task [37].

Inertial sorting of microparticles in microfluidic devices is achieved due to presence of competing shear- and wall-induced lift forces, which are strongly size dependent and hence allowing size based separation as shown in Fig. 2 (d). Inertial focusing based methods have been

particularly useful for achieving high throughput separation of rare cells from blood [44]. A comprehensive review of inertial sorting in straight microfluidic channels can be found in these articles [45,46]. Achieving sorting of more than two particles is challenging in straight microfluidic channels, however spiral microfluidics have been shown to achieve multi-particles sorting as shown in Fig. 2(e). Spiral microfluidics have also been effectively used for ultra-fast and label free isolation of rare cells from blood at ultra-high throughputs [47]. Multi-particle sorting in a spiral microfluidic channel has been achieved by the presence of dean forces in addition to lift forces [39]. The detailed discussions on spiral microfluidics can be found in these articles [39,46]. But these devices still require a sheath flow for multi-particle sorting as reported in Sarkar et al. [48]. Also it is not possible to achieve sorting of similar sized particles with different characteristics using spiral microfluidics, which is doable using techniques such as magnetic sorting by utilizing inherent characteristics such as magnetism.

Lastly, it should be mentioned that most of the above-mentioned passive sorting methods have demonstrated particle sorting in water (Newtonian fluid), however fluids such as blood and saliva used for diagnostics show non-Newtonian behavior. Hence, it is desired that a sorting scheme be devised to achieve separation of multiple particles in non-Newtonian fluids.

1.1.4 Characteristics of an Ideal Sorting Technique

Based on our literature review, we concluded that a sorting technique must have the following characteristics:

(a) It should not require a sheath flow as it dilutes and potentially contaminates the sample and also adds operational complexity to experiments.

(b) It should be done at a high throughput (e.g., 10^9 particles per hour) so that a reasonable sample volume (e.g., >1 mL) can be processed in a timely manner (e.g., within an hour) in order to extract detectable levels of rare targets.

(c) It should have a simple design and the process of fabricating the device should not be complicated.

(d) It should be able to separate particles with high purity (i.e., >90%).

(e) It should be operable without the need for any active external energy so that it could be used in remote areas.

(f) It should be filter-less so as to avoid clogging problem and allow concentrated mixtures to be handled efficiently.

(g) It should be efficient in sorting more than two particles at a time.

(h) It should be capable of separating particles suspended in non-Newtonian fluids too because the biological fluids such as blood and saliva are non-Newtonian.

1.1.5 Objectives of the Thesis and Chapters Organization

Several desired characteristics of an ideal sorting method have been outlined in the previous section, hence the goal of this thesis was to devise a microfluidic technique to achieve sorting of microparticles which complies with these requirements. A hybrid method of sorting was developed by integrating magnetophoresis, inertial or elastic focusing, and pinched flow fractionation into a single device. This combination enabled taking advantage of one method to counter the shortcomings of the others, and hence fulfilling most of the desired attributes of an ideal sorter. To achieve our goal, the objectives of this thesis were to:

1. Devise a sheathless method for pre-focusing and hydrodynamic fractionation of microparticles (using magnetic forces) in a straight microchannel.

2. Investigate the combined effects of inertial, magnetic, and drag forces on microparticles in Newtonian fluids in the abovementioned device.
3. Utilize the gained knowledge to achieve fractionation of up to four particles at a time (fourplex sorting) and investigate the achievable fractionation throughput.
4. Understand the effect of fluid viscosity and elastic forces on multiplex sorting if the particles were suspended in non-Newtonian fluids rather than water.

The concept of hybrid fractionation was tested with a mixture of commercially available spherical MPs and NMPs which can easily be transferred to fractionation of microorganisms and cells in the future. However, other factors such as shape of microorganisms are also expected to influence movement of particles in the channel and have not been investigated here. Moreover, the focus of this thesis was to experimentally establish the principle of fractionation and hence analytical and numerical studies of the fractionation procedure shall be investigated in the future to improve our understanding on how inertial, elastic and magnetic forces interact with each other and contribute to sorting of microparticles. We envisage that a better understanding of the underlying mechanism would enable increasing complexity of separation beyond fourplexing at even higher throughputs than 10^9 particles per hour.

The thesis is organized in a manner such that each of the chapters address one or more of the objectives outlined above. Chapter 2 is focused on addressing objective 1, chapter 3 addresses objectives 2 and 3; and chapter 4 provides discussions on objective 4. Chapters 2 and 3 have been submitted as a manuscript for publication and a version of chapter 4 is currently being prepared for submission as a short journal paper. A brief description of experimental work and results attained in each of the chapters is provided below. Each chapter will also include a more thorough introduction section.

Chapter 2: This chapter is focused on development of a sheathless method for achieving magnetic focusing and hydrodynamic fractionation of two MPs in a microfluidic device. We have integrated magnetophoresis with the concept of PFF to achieve sorting of 5 μm magnetic particles (MPs) from 11 μm MPs at a throughput of 10^7 particles per hour. Firstly, sheathless focusing of 11 μm MPs against the wall of a thin microchannel and their subsequent hydrodynamic deflection at an expansion channel was investigated over a wide range of flow rates (0.5 – 5 mL h^{-1}). Then, a mixture of 5 μm and 11 μm MPs was injected into the device at a flow rate of 5 mL h^{-1} to demonstrate their magneto-hydrodynamic fractionation.

Chapter 3: In this chapter, we capitalized on the abovementioned sheathless method and further combined it with inertial focusing to devise a technique for achieving simultaneous fractionation of 5 μm, 11 μm, and 35 μm MPs from 15 μm non-magnetic particles (NMPs) in the same microfluidic device. Fractionation of more than two types of particles solely by inertia or magnetic forces in Newtonian fluids is a challenging task due to the inherent limitations of each technique. By combination of competitive inertial and magnetic forces in a straight microchannel and addition of a downstream expansion hydrodynamic separator, we overcame these limitations and achieved duplex to fourplex fractionation of MPs and NMPs with high throughput and purity. To achieve this, a systematic study was conducted to enumerate the effect of flow rate, channel aspect ratio and particle sizes on the fractionation performance of the device.

Chapter 4: The experiments reported in chapters 2 and 3 were performed with microparticles suspended in water (Newtonian media), however, particles behave differently when suspended in a non-Newtonian viscoelastic solution like blood. Hence, we conducted a parametric study with respect to flow rate and viscosity to delineate the applicability of our multiplex sorting technique in a synthetic non-Newtonian media.

Chapter 5: This chapter is focused on outlining major conclusions and summary of this thesis. We have also outlined the possibility of future works that can be done based on the understanding of particle sorting we gained from the described research.

Chapter Two

2 Magneto-Hydrodynamic Fractionation (MHF) for Continuous and Sheathless Sorting of High-Concentration Paramagnetic Microparticles*

2.1 Introduction

Microfluidic-based particle sorting methods have contributed significantly to the fields of cancer diagnosis [44,49,50], pathogen separation from water samples [17,51,52] and immunomagnetic assays [53] owing to their compelling advantages such as low cost, portability and minimal reagent consumption [54–56]. Several techniques have been devised on microfluidic platforms to achieve sorting such as Pinched Flow Fractionation (PFF) [11,35], hydrodynamic filtration [3], optical sorting [57], dielectrophoresis [58], acoustic separation [26], Deterministic Lateral Displacement (DLD) [59], size exclusion filtration [60] and magnetophoresis [19]. These methods certainly proffer an avenue to refine and purify desired targets from a mixture and have been used for numerous applications as reported in the literature [61–63]. However, design of a robust sorting device remains elusive as these techniques suffer from major drawbacks such as sheath flow requirement, complex design, limited throughput (low particle concentration and or flow rate), and dependency on external active energy sources.

* This chapter has been submitted in whole as a manuscript for publication in *Biomedical Microdevices*.

The PFF method requires a sheath flow as large as 10-30 times the sample flow rate to perform size dependent particle sorting [11,35,64]. Sheath flow is used to focus the particles on different streamlines along the wall of a microchannel for achieving separation at a downstream expanded channel. The sheath flow is highly undesirable for sample handling as it adulterates and dilutes the sample, hence making recovery of pristine sample a challenging task [65]. Hydrodynamic Filtration (HDF) [3,66], alike PFF, utilizes a laminar flow profile in a microchannel to achieve size based separation, but the efficiency of separation is poor and it works at a throughput of 10^5-10^6 particles per hour. The process of micro-fabricating delicate and size-sensitive micro-posts required for separation using DLD technique is challenging [42]. Microfabricated filters have also been deployed for achieving size-based separation by controlling the size of pores [67]. However, filter-based methods along with HDF and DLD techniques are inefficient at handling concentrated samples due to frequent clogging of particles in these devices. Inertial microfluidic devices have been developed for performing size-based separation of cells and particles, however, their performance is highly restricted by the flow rate and geometry of the channel [45]. The dielectrophoretic, acoustic and optical sorting methods require active external energy sources for operation and hence costly and complex to be adopted [8,21,28].

The magnetophoresis method using permanent magnets [68,69], although not requiring an active energy source, is marred by issues such as low throughput, requirement of sheath flow and complicated fabrication process. Xia et al. [70] used a sheath flow to separate MPs from NMPs at a low flow rate of 30-40 µl h^{-1}. The NMPs were retained confined within the sheath region while MPs were allowed to deflect away from the sheath flow stream owing to magnetic forces acting on them, hence leading to their separation from NMPs. Pamme et al. [14] performed free flow magnetophoresis for separation of 2 µm and 4.5 µm MPs but they also used buffer flow in

order to operate this device. Adams et al. [18] used embedded ferromagnetic stripes to capture and deflect MPs for achieving separation. But their method also required a sheath flow of about ~42 mL h^{-1} when the sample flow rate was ~5 mL h^{-1}. The concentrations of MPs used in their experiments were 0.006%-0.02% of the total mixture, rest being NMPs which amounted to a throughput order of ~10^5 MPs per hour. Embedding the magnetic strips also added another layer of complexity to fabrication of their device.

In this chapter, we report a hybrid sorting method combining magnetic focusing and hydrodynamic separation (called Magneto-Hydrodynamic Fractionation (MHF)) that is able to address the above-mentioned limitations of sorting techniques. We used a very simple design that consisted of a narrow microchannel with one input for sample injection (no sheath flow), a side magnet for sheathless focusing of MPs onto the microchannel wall just like PFF, and a downstream expanded channel for hydrodynamic sorting of focused particles. We firstly characterized the magnetic focusing of 11 µm MPs along the wall of the narrow microchannel over a wide range of flow rates (0.5 to 5 mL h^{-1}) to identify and avoid the flow rates at which the particles start to shift away from the sidewall due to inertial lift forces. Using the concept of MHF, we injected both 5 µm and 11 µm MPs at high concentrations simultaneously into the device and found them aligned at the wall on distinct streamlines because of the difference in their sizes. The distance between these streamlines were further amplified when the magnetic particle were allowed to enter into the expansion zone of the device, leading to their hydrodynamic separation. The throughput of this sheathless hybrid sorting method was 10^7 MPs per hour and on-chip fractionation purity was greater than 98%, both of which have not been achievable with the existing magnetic sorting techniques.

2.2 Materials and Methods

2.2.1 Materials

Silicon wafer (4 in diameter) was obtained from University Wafers Corp (MA, USA). Negative SU-8 2035 photoresist was obtained from Microchem Corp. (MA, USA) and polydimethylsiloxane or PDMS (Sylgard 184) was obtained from Dow Corning (MI, USA). Tween 20 was obtained from Sigma Aldrich (MO, USA). Polystyrene MPs of mean diameter 5 µm and 11 µm were obtained from Spherotech Inc. (IL, USA). The N42 grade permanent magnet that was used in all experiments was obtained from Indigo Instruments (ON, Canada). The magnets were cuboid with length of 25 mm, width of 10 mm and height of 2.5 mm. Masterflex® Tubing and interconnects used for device operation were acquired from Cole Parmer (QC, Canada) and Qosina Corp. (NY, USA), respectively.

2.2.2 Particle Suspensions

The stock solutions of 5 µm and 11 µm diameter MPs had a size distribution of 4-5 µm and 10-13.9 µm, respectively. The suspension of particles used for experimentation had a number density ratio of 10:1 for 5 µm and 11 µm MPs, respectively, and concentration of the mixture was about 1.1×10^7 particles per mL. The density of particles were approximately 1.05 g cm^{-3}, almost the same as water density. Hence, the sedimentation velocity of these particles were negligible compared to their flow velocity in forward direction. All particle suspensions used in this study were prepared in DI water. A small amount of Tween 20 (~0.1 wt %) was added to particle suspension to avoid any possible particle aggregation and to keep them dispersed in the sample.

2.2.3 Device Design

The MHF microfluidic particle sorting device is shown in Fig. 3. It consisted of two regions, namely the magnetic focusing zone and the hydrodynamic expansion zone. The magnetic focusing zone was designed as a narrow microchannel ($L_{Focusing\ Zone}$= 40 mm, $W_{Focusing\ Zone}$= 90 µm, L_o= 2 mm, and W_o= 55 µm) over which the MPs were attracted towards a permanent magnet located by the side of the channel. The length of the focusing zone was designed based on existing guidelines for lateral movement velocity of MPs to ensure that they remain under the effect of magnetic force for a long duration to get focused against the wall at the highest flow rate of 5 mL h^{-1} tested in our experiments [71]. The width of focusing zone was chosen to be 90 µm so that it was wide enough to avoid any chance of clogging of 5 µm and 11 µm MPs in the channel. The hydrodynamic expansion zone ($L_{Expansion\ Zone}$= 30 mm, $W_{Expansion\ Zone}$= 11 mm) was designed to increase the separation distance between the magnetically focused particles and image them downstream of the device when the flow from the focusing zone was completely stabilized. The height of channels were all 50 µm.

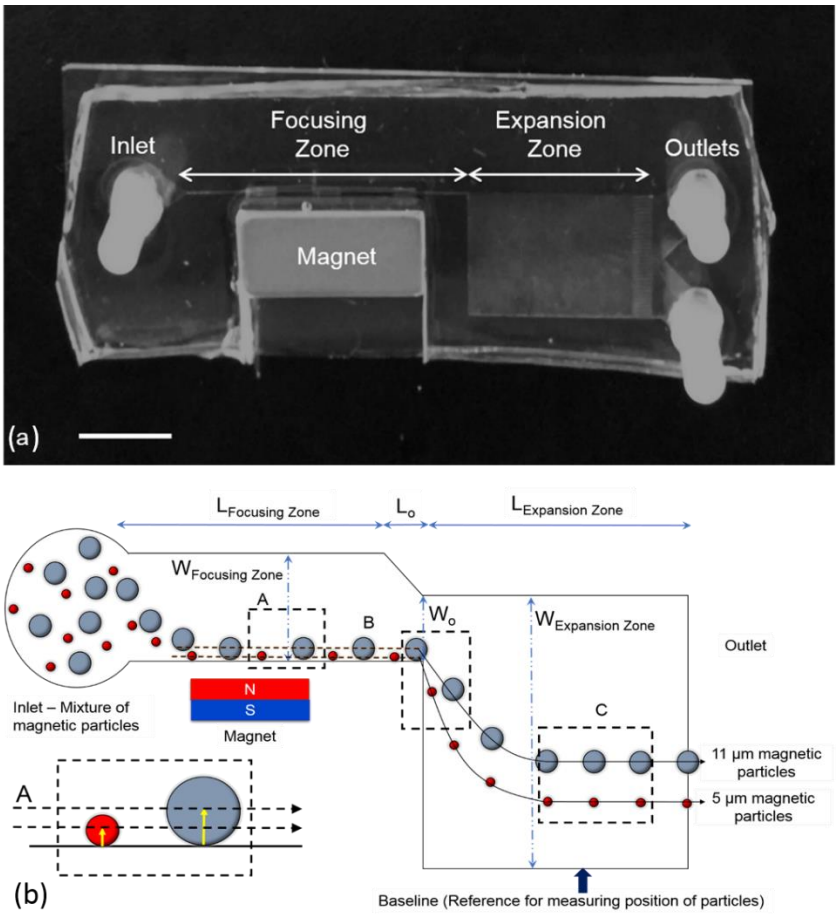

Figure 3. *(a) Image of the MHF microfluidic particle sorting device (Scale bar = 10 mm). (b) Schematic of the MHF device showing separation of 5 µm and 11 µm MPs based on the concept of magnetic focusing and hydrodynamic fractionation.* $L_{Focusing\ Zone}$ *= 40 mm,* L_o *= 2 mm,* $L_{Expansion\ Zone}$ *= 30 mm,* $W_{Focusing\ Zone}$ *= 90 µm,* W_o *= 55 µm,* $W_{Expansion\ Zone}$ *= 11 mm, Height of channel = 50 µm.*

2.2.4 Device Fabrication

The devices in this chapter, and rest of the chapters, were all fabricated using standard photo- and soft-lithography methods and a detailed procedure can be found in McDonald et al. [72]. Briefly, SU-8 photoresist was spun over a 4 in silicon wafer and exposed to ultraviolet light via a photomask that contained the microchannel design discussed above and shown in Fig. 3. The process was then followed by heat curing and dissolving the unexposed SU-8 in developer solution to get the master mold. Then, PDMS pre-polymer mixture of base and curing agent in

the ratio of 10 to 1 was thoroughly mixed and degassed in a vacuum chamber. The mixture was poured over the silicon master mold with the permanent magnet put in place, and allowed to cure for 2 h at 80^{o}C. The cured PDMS layer was peeled off the mold and bonded against a glass slide using oxygen enhanced plasma bonding to obtain the final device. The bonded device was further kept for 1 h at 80^{o}C to enhance the bonding.

2.2.5 Experimental Setup and Procedure

The microfluidic device was connected to a 10 mL syringe via a connecting tube at the inlet. The syringe was operated with a pump (Legato 110, KD Scientific, USA) to apply the desired flow rates (0.5 – 5 mL h^{-1}). The device was first washed with de-ionized water for 10 minute before introducing the particle suspensions into it. Then, particles were injected into the device and flow was allowed to stabilize for 15 minutes. We observed focusing and fractionation upon introducing the particles into the channel, however, we allowed this lag time for the sake of getting more reliable results. The device was kept under an inverted microscope (Bioimager, ON, Canada) and a camera (Point Grey, BC, Canada) was installed on it to capture the images and videos of particles sorting at regions B and C of the device.

2.2.6 Data Analysis

The number of particles distributed in regions B or C of the channel (Fig. 3b) were quantified using freeware ImageJ. Each recorded image was subdivided into a series of frames of a specific height with reference to the baseline depicted in Fig. 3b. The particles in each frame were counted using “analyse particle” function of ImageJ and plotted against their position to get a quantitative representation of the distribution of particles in the device. The width of these frames ranged from 50 µm to 350 µm dependent on the distribution of particles along the width of the channel, i.e., the denser the particles distribution the thinner the selected frames. In our

duplex sorting experiments, the number of 5 μm MPs found mixed with the 11 μm MPs at the boundary of stream of these MPs were counted and used to calculate the fractionation purity of our device. Although we intended to provide feasibility and design guidelines in this study and did not implement separate outputs to extract the sorted particles from our device, but this task can be easily performed by splitting the outlet channel at desired locations.

2.3 Working Principle

The sorting method shown in Fig. 3b is a hybrid two-step process involving magnetic focusing of MPs of different sizes inside a narrow microchannel followed by their hydrodynamic separation inside a downstream expansion region. In the first step, the randomly distributed MPs in the inlet are attracted towards the magnet and aligned along the inner wall (region A in Fig. 3b) of the channel close to the magnet. The success of this step is critical, otherwise separation cannot be achieved in the device. As discussed in the Materials and Methods section, it is important that the competing magnetic and drag forces acting on the particles and the focusing channel geometry [71] are considered in the device design, in order to ensure attracting and capturing all the particles at the sidewall of the channel right before they enter the expansion zone. Inertial forces in microfluidic channels have been demonstrated to shift particles away from the channel walls [45,73], hence it is important to ensure that the magnitude of inertial forces are not dominant in MHF such that particles get focused away from the walls. With minimized inertial forces, magnetic alignment forces the particles to focus on specific streamlines corresponding to the distance of their geometric centers to the channel sidewall (assuming that the particles are ideally spherical and mono-sized). In this case, the 5 μm and 11 μm MPs align on different streamlines because of differences in their sizes as shown in region A of Fig. 3b. When these distinct streamlines enter into the expansion zone (region B of Fig. 3b), they get hydrodynamically

separated from each other leading to size-based sorting of the MPs in region C. With the hydrodynamic expansion section, the need for extended channel lengths or microfabrication of magnetic field gradient generators to achieve distinct separation bands of MPs in existing magnetophoretic separation microdevices can be easily avoided.

2.4 Results and Discussion

2.4.1 Magnetic Focusing of Paramagnetic Microparticles

As discussed in section 2.3, achieving focusing of MPs against the inner sidewall of the microfluidic device (at region B in Fig. 3b) is the first and most crucial step towards the sorting process. Hence, we investigated the behavior of 11 μm MPs over a wide range of flow rates (1–5 mL h^{-1}) in the device. The experiments were performed under two conditions, one without any magnet and the other with the magnet positioned along the inner wall of the narrow microchannel. The experiments performed without any magnet in the setup showed that particles were randomly distributed in the channel at flow rates below 5 mL h^{-1} as shown in Fig. 4a (depicting region B of the device). Particles were observed to be weakly focused in the channel as the flow rate was increased to 5 mL h^{-1}. This can be attributed to weak inertial forces that caused the particles to focus at the center of the channel [45,74]. On the other hand, a strong focusing against the sidewall was observed at all flow rates when a magnet was introduced into the setup. Essentially, the MPs were attracted towards the magnet and aligned themselves along the wall. Fig. 4b shows the magnetically focused particles at all flow rates after being deflected into the expansion zone (region B in Fig. 3b) of the device. This study helped us ascertain that in the range of flow rates tested, the effect of magnetic focusing of particles against the sidewall was always dominant over inertial focusing in the center.

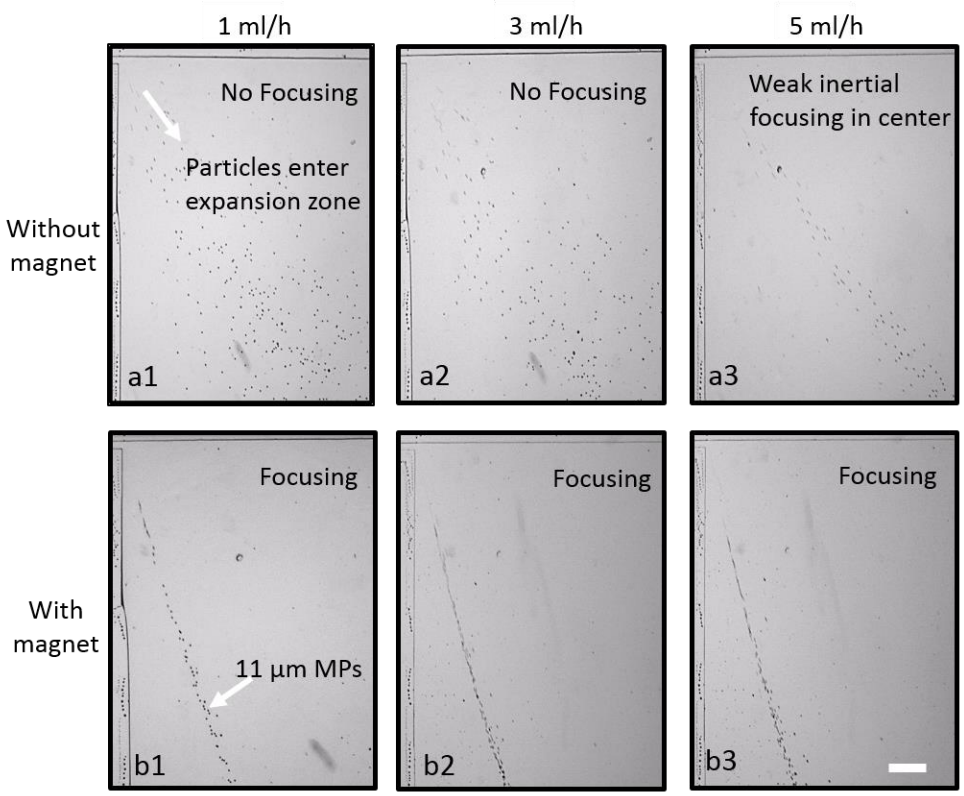

Figure 4. *The images on top (a1-a3) show distribution of 11 µm MPs in the entrance to expansion zone (region B) without any magnet in the setup, and the images at the bottom (b1-b3) show corresponding focusing of 11 µm particles after introducing the magnet into the setup. (a1) and (b1) were taken at a flow rate of 1 mL h^{-1}, (a2) and (b2) were taken at a flow rate of 3 mL h^{-1}, while the flow rate for (a3) and (b3) was 5 mL h^{-1}. Scale bar = 250 µm. The flow direction was from left to right in all images.*

We also quantified the position of particles downstream the flow in region C of the device in order to illustrate the behavior of particles with and without the magnet as observed in Fig. 4. For this, the position of particles were measured with respect to the baseline shown in Fig. 3b. We divided the images acquired from region C into bands of 350 µm-thick frames assuming baseline as the reference. The number of particles exiting from each band was then counted and the fraction of particles at each band was acquired by dividing the number of counted particles by the total number of particles that went through the device. Fig. 5 shows the results for experiments performed at 3 mL h^{-1} (Fig. 4, a2 and b2) for 11 µm particles in the channel. The

black blocks in Fig. 5 represent distribution of magnetically focused particles while the white blocks demonstrate the random distribution of the particles along the width of the channel when no magnet was used in the setup.

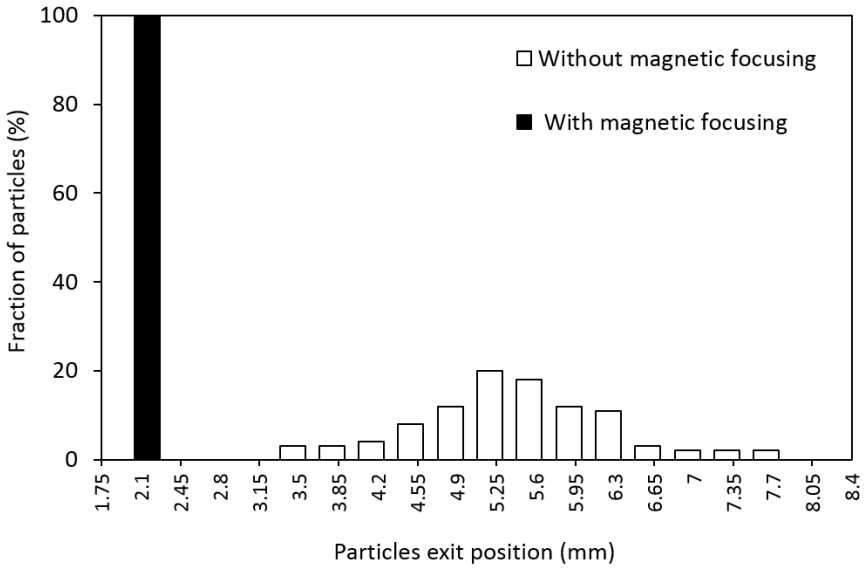

Figure 5. *Fraction of 11 µm particles flowing at 3 mL h^{-1} in the device and getting distributed along the width of the expansion zone and away from the baseline (i.e., lower wall of expansion zone). The white blocks show the distribution of particles when they were injected into the device without any magnet and hence, they were found randomly distributed. The black block shows the distribution of particle when magnet was introduced into the setup. The particles were found strongly focused and shifted towards the wall of the channel. Each block corresponds to a window of 350 µm across the width of the expansion zone.*

We found that the MPs, without a magnet in the setup, were dispersed over the region 3.5-7.35 mm away from the baseline. However, they were found concentrated, when the magnet was introduced into setup, within a small region 2.1-2.4 mm away from baseline. The results in Fig. 4 and Fig. 5 clearly demonstrate that the concept of magnetic focusing could be used for manipulation of particles inside an expanding microchannel hence eliminating the need for diluting sheath flows used in the conventional PFF and magnetophoresis techniques [11,14].

2.4.2 Effect of Particle Velocity on Magnetic Focusing Position and Efficiency

As discussed in section 2.3, we intended to minimize the effect of inertial focusing in MHF in order to investigate the effect of magnetic focusing and hydrodynamic deflection in this technique. Accordingly, we present the effect of velocity on magneto-hydrodynamic deflection position and focusing efficiency of particles in this section. The experiments were performed with 11 µm MPs in the presence of the magnet in the device and flow rate was varied from 0.5 to 5 mL h^{-1}. Since visualizing the focusing efficiency of particles in the narrow channel was not possible due to particles' high velocities, we imaged them in region C of the device (Fig. 3b) where the particles velocity slowed down. As shown in Fig. 6a, we observed that there was a slight shift in the focusing position of particles towards the center of the channel as the flow rate was increased. The focusing position of particles moved away from the baseline at higher velocities but this dislocation was lower than 5% of the total width (11 mm) of the expansion channel. Fig. 6b shows that the mean position of focused particles at 0.5 mL h^{-1} was approximately 1.8 mm away from the baseline, while the mean position of focused particles at 5 mL h^{-1} was approximately 2.3 mm away from the baseline. This small shift in focusing position can be explained with the help of the fact that particles in a microchannel experience weak inertial lift forces towards the center of the channel and this force increases with increase in velocity [45,75]. A similar observation was made in several other reports, where it was found that particles experience a weak wall induced lift force and hence shift away when they were focused against the walls of a channel using a sheath flow in conventional PFF methods [73]. We also calculated the 11 µm MPs particle Reynolds number in the channel (Re_p=0.4 at 5 mL h^{-1}) as an evidence to ensure that the effect of inertia in our method was insignificant (i.e., Re_p<1)

[45,76]. MHF at flow rates higher than 5 mL h^{-1} must be performed with caution and upon applying design modifications to the channel geometry to control the effect of inertial focusing.

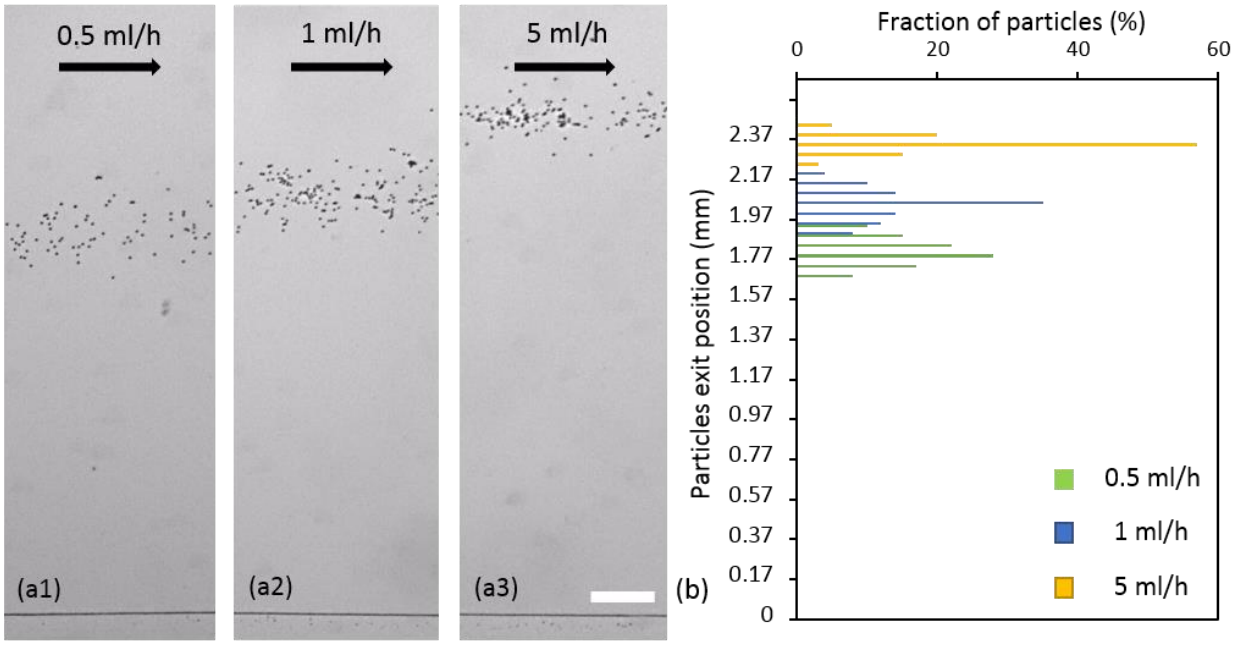

Figure 6. *(a1-a3) Effect of flow rate on position of 11 µm particles after magnetic focusing and deflection in the channel at region C of the device. It is clear that the position of particles with respect to the baseline is changing with velocity. It was observed that particles shifted away from the wall with displacements smaller than 5% of* $W_{Focusing\ Zone}$*, as flow rate was increased from 0.5 to 5 mL* h^{-1}*. Scale bar = 250 µm. The flow direction was from left to right in all images. (b) The plot of exit position of magnetically focused particles at different velocities. Green, blue and yellow blocks show distribution of particles at 0.5 mL* h^{-1}*, 1 mL* h^{-1} *and 5 mL* h^{-1} *flow rates, respectively, with quantitative demonstration of inertial shift in particles' position.*

It is worth noting that this study also provided an insight into the quality of particles' focusing in the channel. At lower flow rates (e.g., 0.5 mL h^{-1} in Fig. 6), it was observed that the particles were more dispersed along the width of the channel as compared to their more focused distributions at higher flow rates (e.g., 5 mL h^{-1} in Fig. 6). About 40% of particles were located in a 100 µm window at 0.5 mL h^{-1}, while almost 80% of particles were concentrated in a 50 µm window at 5 mL h^{-1}. This clearly indicated that although the effect of inertia was not dominant to

displace the stream of particles in the device, but it was strong enough to induce a desirable particle band focusing in MHF. Accordingly, the optimum focusing and deflection flow rate of 5 mL h^{-1} was selected for sorting of MPs of two different sizes in the device.

2.4.3 Magneto-Hydrodynamic Fractionation of 5 µm and 11 µm Paramagnetic Microparticles

We investigate the performance of the device in MHF of particles based on their sizes in this section. We chose to work with a mixture of two MPs of 5 µm and 11 µm diameter. Firstly, the mixture of both particles was injected into the device at a flow rate of 5 mL h^{-1} and particles distribution was observed in the expansion region B of the device. Fig. 7a shows that particles were randomly distributed and completely unsorted in the device when no magnetic focusing was performed in the narrow channel. We then repeated this study under the same conditions with a magnet by the side of the channel. The distribution of both particles in the expansion zone in this condition is presented in Fig. 7b. It was found that both particles were magnetically focused in the device. Furthermore, the streams of 5 µm and 11 µm MPs were also separated from each other. Essentially, the difference in size between 5 µm and 11 µm particles made them lie on different streamlines and they got hydrodynamically separated upon entering into the expansion zone.

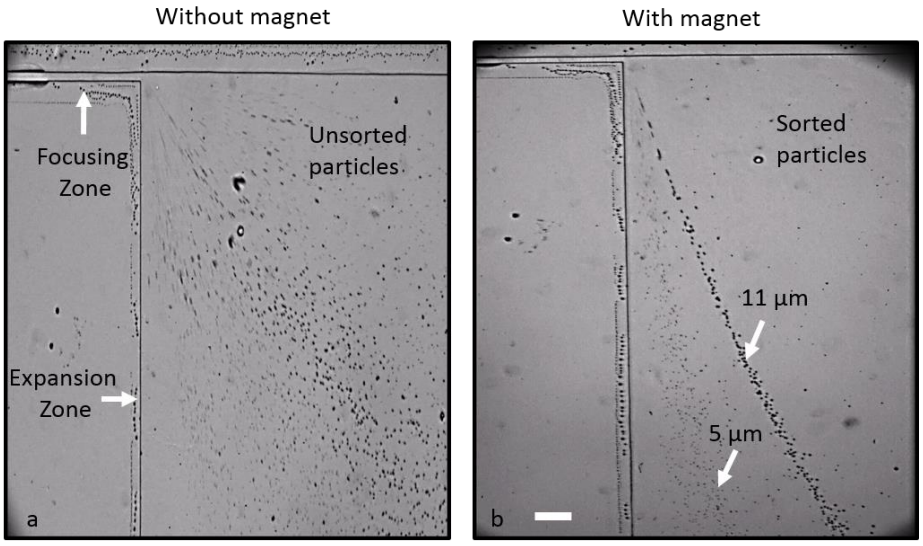

Figure 7. *Duplex particle separation in the hybrid MHF microfluidic sorter. (a) Both 5 µm and 11 µm particles were simultaneously injected into the device without any magnet and a random distribution of particles was observed. (b) The distribution of particles at the same location in expansion zone after adding a magnet into the system. It was found that both particles were focused and separated from each other. The flow rate for this experiment was 5 mL* h^{-1}*. Scale bar = 250 µm. The flow direction was from left to right in both images.*

The deflected streams of particles in Fig. 7b were found to be distributed over distinct positions downstream of the flow. Fig. 8a shows the observed distribution of sorted particle in region C of the device downstream from the expansion zone. We quantified the position of particles using the same process discussed in this chapter and the particles were counted over windows of 100 µm width. Fig. 8b shows the distribution of both particles along the width of the expansion zone and with the magnet in the setup. It was found that 11 µm MPs were distributed over a region extending from 2.1 mm to 2.5 mm away from baseline. On the other hand, the 5 µm MPs were closer to the wall and distributed over a region from 0.2 to 2.1 mm away from the baseline.

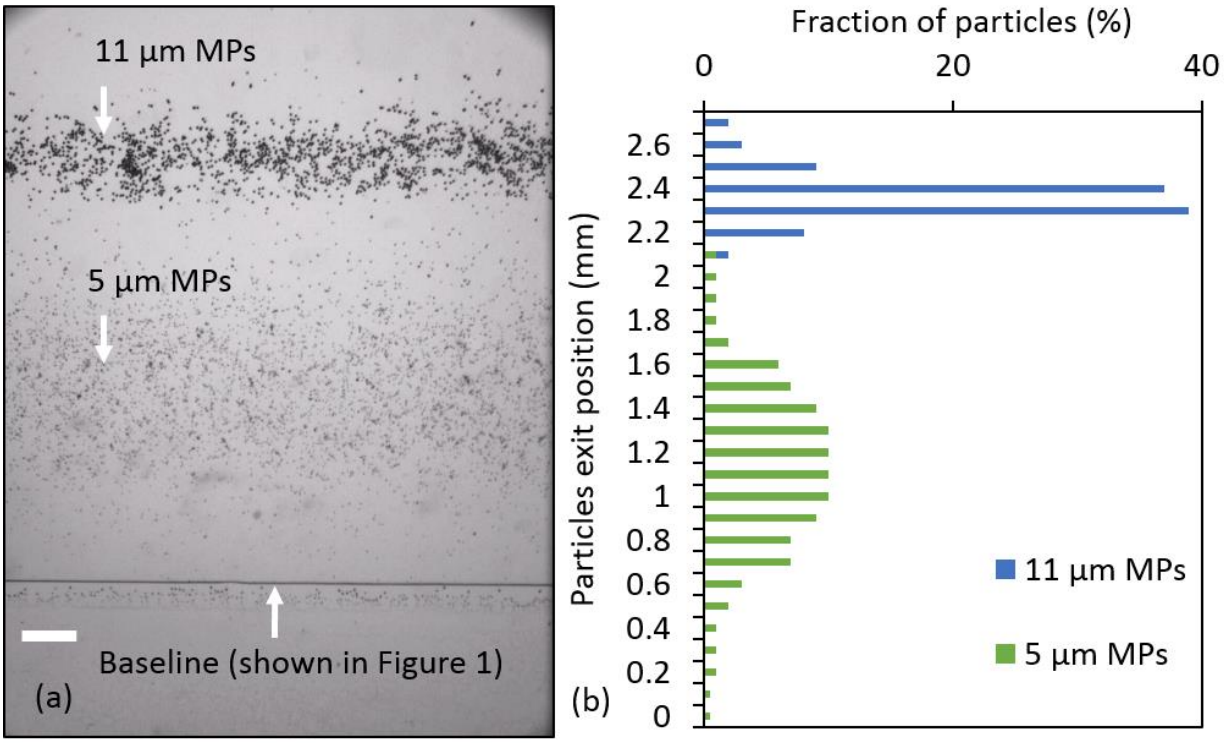

Figure 8. *(a) Separation of 5 µm and 11 µm MPs at 5 mL h^{-1} flow rate observed at region C of the device. Scale bar = 250 µm. The flow direction was from left to right. (b) The particle distribution in (a) was quantified by counting the particles over windows of 100 µm width. The 5 µm MPs (represented by green blocks) were observed to be well separated from 11 µm MPs (represented by blue blocks).*

The on-chip fractionation purity was estimated by calculating the fraction of MPs mixed together at the boundary of their streams. As shown in Fig. 8b, approximately 2% of the total 11 µm MPs in the device were mixed with 1% of total 5 µm MPs at a distance 2.1 mm away from baseline, leading us to conclude that the purity of fractionation was approximately 98%. The throughput of this sorting method was estimated to be around 5×10^{7} particles per hour as the concentration of mixture of particles used for this study was approximately 1.1×10^{7} particles per mL and flow rate was maintained at 5 mL h^{-1}. The throughput achieved by the existing magnetophoretic sorting methods is in the order of 10^{3}-10^{6} particles per hour at purities over 90%. Our method not only

improves upon these characteristics, but also provides sheathless sorting that has not been achievable with the existing methods. [14,18,70]

As shown in Fig. 8, 5 µm MPs were distributed over a wider region compared to 11 µm MPs. This can be potentially attributed to 3D migration of particles to preferable equilibrium positions along the height of the microchannel in a laminar flow. It has been reported that microparticles in a rectangular microchannel (width>height) quickly tend to occupy equilibrium inertial positions at top and bottom of the channel because of shear and wall induced lift forces [74]. However, these forces are strongly size dependent [46,77]. We believe that 5 µm and 11 µm MPs assumed different positions height-wise in the device after magnetically getting focused onto the sidewall of the channel, right before entering the expansion zone, as shown schematically in Fig. 9. We hypothesize that the smaller 5 µm MPs were less likely to assume any favorable inertial equilibrium position in the focusing zone of our device, and were rather distributed throughout the channel sidewall during magnetic focusing. But, the 11 µm MPs were more likely to focus inertially on two equilibrium positions in the channel while being magnetically pulled towards the sidewall. Hence, because of the 3D paraboloid nature of velocity profile in a rectangular cross-section, the 11 µm MPs would follow symmetric streamlines while the 5 µm MPs would lie on various ones. Consequently, 5 µm MPs were distributed over a larger region compared to 11 µm MPs, when these streamlines entered into the expansion zone. This however did not interfere with separation of particles and sorting was still attainable with high throughput and purity.

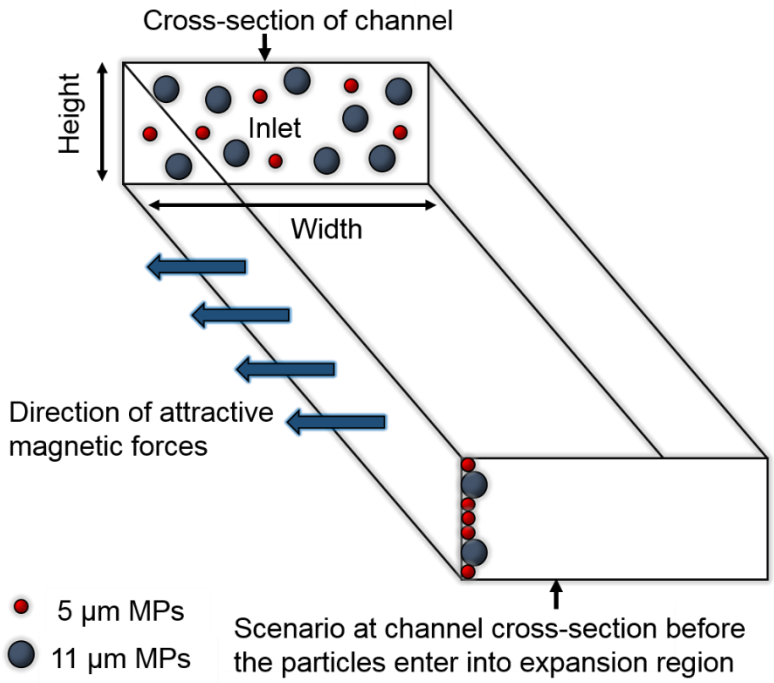

Figure 9. *Expected distribution of particles at cross-section of the channel in the magnetic focusing zone for 11 µm and 5 µm MPs. The 11 µm MPs are inertially focused at two equilibrium positions along the height of the channel while 5 µm MPs are not experiencing any significant inertial forces because of their smaller size. Hence, 5 µm MPs do not get focused at any preferable position and are distributed throughout the height of the channel. Both of these particles were attracted towards the wall because of attractive nature of magnetic forces and hence were envisaged to be arranged as shown just before entering the expansion zone of the MHF device.*

2.5 Conclusions

We have developed a novel hybrid method for sorting of magnetic microparticles which can be used for separation of particles and biological cells (based on their inert magnetic properties or by immunomagnetic tagging) based on their size and magnetic characteristics. This method of sorting offers sheathless operation and simple design. It does not require any external active energy source while working at a high throughput (10^7 particles per hour) and performing separation with high fractionation purity (98%) which has not been achieved by existing duplex magnetophoretic methods. It was also found that particles aggregate when passing through

expansion zone of the device due to reduction in linear flow velocity, however these aggregates do not exhibit any cross-stream movement and hence the stream of 5 and 11 μm magnetic particles analyzed using ImageJ should not lead to any uncertainty in calculations. This sorting device can be used to separate two particles of different sizes, however a better performance would be observed when there is a larger difference in the sizes of particles. Combination of this approach with inertial focusing at higher flow rates will lead to separation of multiple magnetic and NMPs at even higher throughputs.

Chapter Three

3 Multiplex Inertio-Magnetic Fractionation (MIMF) of Magnetic and Non-Magnetic Microparticles in a Microfluidic Device[†]

3.1 Introduction

Separation of small substances such as micro- and nano-particles, amino acids, and cells distinctly from a heterogeneous sample is critical for many applications such as cellomics [78], genomics [79], diagnosis [80,81], and immunoassays [82]. Fluorescence-Activated Cell Sorting (FACS) [83] is one of the most commonly used methods for sorting targets based on their fluorophore labelling. But FACS needs compatibility of targets with fluorescent tagging and requires in-line fluorescent imaging, analysis and active downstream sorting that makes the technique complex, expensive and inaccessible. Several microfluidic-based methods such as Deterministic Lateral Displacement (DLD) [59], Pinched Flow Fractionation (PFF) [11] and spiral microfluidics [84] have been developed to execute multi-particle sorting. DLD method works at low throughput and its performance is marred by the frequent clogging of particles in the device. The PFF method also works at very low throughput and cannot be operated without a diluting sheath flow. Spiral microfluidic devices can be used for multiplex sorting (e.g., fourplex

[†] This chapter has been submitted in whole as a manuscript for publication in *Microfluidics and Nanofluidics*.

sorting in [85]) but the technique still requires a high ratio of sample to sheath flow and its operation is highly constrained by the geometry of the channel and limited to a narrow range of flow rates. Moreover, DLD, PFF, and spiral microfluidic sorting methods have a common limitation of sorting particles solely based on the difference in their sizes which means that sorting of two particles with identical or very close sizes but different inherent characteristics such as magnetization cannot be achieved with these methods.

To address the limitations above, the magnetophoretic separation technique has received a significant attention. Magnetic sorting has unique operational advantages as it is reasonably unperturbed by changes in medium temperature or particle characteristics such as surface charge and ionic concentration [86]. Miltenyi et al. [87] used macroscale chromatographic columns for separating magnetically-labelled targets from non-magnetic entities in late 1980's while naming the technique Magnetic-Activated Cell Sorting (MACS). Since then, the magnetophoretic technique has been implemented in microfluidic devices, for instance, to achieve separation of two similar-sized particles based on the difference in their magnetic properties [88]. Over the past two decades, microfluidic-based magnetophoretic separation has showed a great potential for development of cost-effective and portable particle sorting technologies with some simpler systems already making their way to the market by companies such as Miltenyi Biotech and BioLegend. However, achieving multiplex sorting of MPs and NMPs at high throughput and without the need for a sheath flow still remains a challenge in this field.

It has been reported that generation of a high-gradient magnetic field (HGMF) [89] inside microfluidic devices and close to the stream of particles can improve the magnetic sorting performance significantly. HGMF in microfluidic devices can be generated by integration of soft magnetic materials inside microchannels, magnetized either by electromagnets or by permanent

magnets. Rong et al. [15] developed an on-chip magnetic bead sorter using six solenoid type micro-inductors for sorting and transferring 8μm magnetic particle from an input stream to a collection outlet in the device. However, they reported that the sorting of magnetic beads was possible only at a low flow velocity of 60 μm h^{-1}. Xia et al. [70] demonstrated sorting of 1.6 μm MPs from 2 μm NMPs at a throughput of ~10^6 particles per hour using a needle or comb shaped HGMF concentrator made from NiFe (80% Nickel, 20% Iron). Giudice et al. [90] demonstrated two-particle sorting, i.e., 6 μm or 20 μm NMPs from 10 μm MPs, dispersed in a viscoelastic solution with a separation efficiency of up to 96%. The technique required an external buffer flow for sorting and the maximum flow rate of operation was 240 μl h^{-1}. Tsai et al. [91] demonstrated separation of 0.5 μm MPs from 1.6 μm MPs using a permanent magnet in a straight microchannel, however a sheath flow for performing separation was again required in their device. Inglis et al. [88] embedded nickel magnetic stripes into a microfluidic channel and magnetized them using an external permanent magnet for separating two targets at a flow velocity of 240 μm s^{-1}. The particles had to be aligned with a sheath flow and the process of fabricating the magnetic stripes in the narrow microchannel is relatively complex. Recently, we demonstrated a method for size-based fractionation of 5 μm MPs from 11 μm ones in a microfluidic device [92]. This hybrid technique was devised based on a combination of magnetic focusing of particles against the wall of a microchannel and their hydrodynamic fractionation downstream which required no sheath flow and could be operated at a flow velocity of 0.3 m s^{-1}, which was significantly higher than majority of abovementioned methods.

Several attempts have been made to separate more than two particles in magnetophoretic devices to address the technological need of multiplex fractionation in handling complex mixtures such as blood and water. Adams et al. [18] demonstrated triplex sorting and separated two MPs from a

NMP, using a similar technique as reported by Inglis et al. [88]. Essentially, they fabricated two regions of magnetic strips in their microchannel for deflecting MPs at different angles into two collection channels and restricted NMPs from entering into collection outlets using an excessive sheath flow. Chalmers et al. [93] used magnetic dipole and quadrupole to separate targets based on their extent of magnetic labelling at a throughput of ~10^6 particles per hour. Pamme et al. [14] performed continuous triplex sorting and separated 2 µm and 4.5 µm MPs from 6 µm NMPs using a sheath flow to focus the particles in a channel with a side-channel magnet to sort the particles at a throughput of ~720 particles per hour. All in all, current magnetophoretic based particle sorting techniques can achieve triplex sorting at low flow rates while suffering from shortcomings such as a need for sheath flow and fabrication of delicate micro-strips to achieve HGMF in the channel.

In this chapter, we introduce a novel hybrid technique called Multiplex Inertio-Magnetic Fractionation (MIMF) to simultaneously fractionate up to four microparticles in water at a throughput of 10^6-10^9 particles per hour. MIMF is based on interaction between inertial and magnetic forces for achieving fourplex fractionation of microparticles in a microchannel. In comparison to our duplex method [92]that was capable of fractionating 10^7 MPs per hour at low flow rates (magnetic force dominance), MIMF can fractionate MPs from each other and from closely-sized NMPs (duplex to fourplex) at several orders of magnitude higher throughputs by taking advantage of inertial forces that become dominant in our device upon optimizing geometry and at desirably higher flow rates. We firstly conducted a comprehensive parametric study to investigate the effect of flow rate, channel aspect ratio and particle size on duplex MIMF to understand the behavior of particles in our device. We then used the obtained knowledge to demonstrate triplex and fourplex MIMF of MPs and NMPs in the device at high

throughputs and fractionation efficiencies. We anticipate adoption of MIMF in immunomagnetic separation applications in which multiple target biological substances such as biomolecules, cells, and microorganisms need to be tagged and separated in various types of fluids.

3.2 Materials and Methods

3.2.1 Microparticles and Materials

Polystyrene magnetic beads referred to as 5 µm (size distribution of 4-4.9 µm) and 11 µm (size distribution of 10-13.9 µm) MPs were obtained from Spherotech Inc. (IL, USA). The 35 µm polyethylene MPs (size distribution of 32-38 µm) were procured from Cospheric LLC (CA, USA). The polystyrene NMPs used in this study had an average size of 15 µm (size distribution of 10-19 µm) and were obtained from Phosphorex Inc. (MA, USA). We intentionally chose to work with poly-dispersed non-MPs due to two reasons. First, to use them as surrogates for a variety of non-target non-magnetic materials (e.g., cells of different sizes) in the future application of MIMF in immunomagnetic separation of multiple magnetically-tagged target analytes from non-targets and the solution. Second, to demonstrate that two closely sized particles, one magnetic (10-13.9 µm) and one non-magnetic (10-19 µm) could also be fractionated in our device at high throughput and efficiency.

Silicon wafers and SU-8 2035 photoresist required for device master mold fabrication were procured from Wafer World Inc. (FL, USA) and MicroChem Corp. (MA, USA), respectively. Polydimethylsiloxane or PDMS (Sylgard 184 kit) for soft lithography-based replication of MIMF microfluidic devices was obtained from Dow Corning Corp. (MI, USA) and Tween 20 was procured from Sigma Aldrich (MO, USA). N42 grade cuboid magnet (length 25 mm, width

10 mm and height 2.5 mm) used for magnetic separation of particles in the MIMF device was obtained from Indigo Instruments (Waterloo, ON, Canada).

3.2.2 Design and Fabrication of MIMF Device

The experiments were performed in the device shown in Fig. 3. We fabricated microchannels with various heights (30, 40, 50 and 60 μm) to investigate the effect of Aspect Ratio (AR=Width/Height) and hence inertial forces [94–96] on MIMF. The focus of this chapter was to investigate the concept of multiplex inertio-magnetic fractionation of microparticles and not sorting, hence only two outlets were implemented in this device. However, the findings can easily be used as a design guideline to add outlets at desirable locations in the channel for future sorting of particles or particle-analyte conjugates (currently under investigation).

3.2.3 Experimental Procedure and Data Analysis

Duplex, triplex, and fourplex mixtures of particles at desirable concentrations (10^4-10^8 particles per ml) in deionized water were prepared off the chip and injected into devices with various geometries using a syringe pump (Legato 110, KD Scientific, USA). The sample input flow rate was varied (1 – 9 mL h^{-1}) to study the effect of flow rate on separation performance in MIMF. There was no need for use of sheath flow in this method. Images and videos of particles distribution were captured at regions B and C (Fig. 3b) of the device using a camera (GS3-U3-23S6C-C, Point Grey, BC, Canada) at a frame rate of 162 frames-per-second, mounted on an inverted microscope (BIM500FL, Bioimager, ON, Canada). Before performing any imaging and as a precaution, we ran the experiments for 15 minutes to allow the flow to stabilize in the device although fractionation was observed within 1-2 minutes of sample injection. The freeware ImageJ was used for analysing the captured images of particles in the device. For quantifying the position of particles, we partitioned the image into a sequence of narrow

windows of 100 μm width and used the "analyse particle" function in imageJ for counting the number of particles in each of these windows.

3.3 Working Principle

For a laminar flow in a circular microchannel, it has been found that spherical microparticles tend to focus at a distance 0.6 times the radius away from the center of the channel [97]. It has been shown that focusing is promoted by net inertial lift forces acting on these particles [12,45]. It has also been reported that particles tend to focus in two central equilibrium positions when flowing in a rectangular channel with AR>1 [74]. The net inertial lift force acting on the particles in the direction transverse to the flow (Fig. 3b) can be expressed as [74]:

$$F_{IL} = C_L \frac{4U_f^2}{D_h^2} \rho a^4 \quad (1)$$

where C_L is lift coefficient, U_f is average flow velocity (m s^{-1}), D_h is hydraulic diameter of the channel (m), ρ is density of the fluid (Kg m^{-3}) and a is the diameter of particles (m). The channel Reynolds number ($Re_c = \rho U_f D_h/\mu$, where μ is dynamic viscosity of fluid in Pa s) and particle Reynolds number ($Re_p = Re_c (a/D_h)^2$) have been used to assess the strength of inertial forces in microchannels [45,76]. It has been highlighted in several reports that inertial forces significantly affect the focusing of microparticles in microchannels when $Re_p \geq 1$, and we shall also be adopting this criterion [23,45] to explain the fractionation of microparticles in our MIMF device. Another dominant force is the stokes drag force (F_D) that acts against the motion direction of microparticles in the channel. The magnitude of stokes drag force can be expressed as [74]:

$$F_D = 3\pi\mu a v \quad (2)$$

where v is the velocity (m s^{-1}) of particles in the lateral direction. Finally, the force acting on a magnetic particle due to a permanent magnet such as the one used in our MIMF device (Fig. 3) can be expressed as [18]:

$$F_M = \frac{4\,\Pi}{3} M\,\nabla B\,a^3 \tag{3}$$

where M is magnetization (A m^{-1}) and ∇B is magnetic field gradient (T m^{-1}). According to equations (1) to (3), MPs are under the effect of magnetic, drag and inertial lift forces, while NMPs are under the effect of drag and inertial lift forces only.

Multiplex particle fractionation is achievable in our MIMF device owing to interaction between magnetic, drag and inertial lift forces. Hypothetically, the device should be capable of focusing NMPs inertially at the center of the channel if $Re_{p,NMP} \geq 1$, while fractionating the MPs across the width of the channel if $Re_{p,MP}$ does not significantly exceed unity so that magnetic and inertial forces act comparatively on these particles. Upon maintaining the magnetic field gradient constant, the movement of particles inside our device would be dependent mostly on input flow rate, channel aspect ratio (or hydralic diameter) and particle sizes. Effects of these parameters have been investigated to devise a fourplex particle fractionation microdevice. Our focus was multiplex fractionation in water so effect of fluid properties was not studied.

3.4 Results and Discussion

In this section, we first parametrically investigate the effects of flow rate, channel aspect ratio and particle size on separation of MPs from NMPs. The outcomes are then used to demonstrate MIMF of three and four particles simultaneously in our device (Fig. 3).

3.4.1 Duplex MIMF and Parametric Studies

As described in Section 3.3, a mixture of MPs and NMPs injected into our device would tend to get inertially focused in the center of the channel in the absence of any magnetic force. However, only MPs will be attracted towards the wall of the channel and get separated from the stream of NMPs upon positioning a magnet in the device (if $Re_{p,MP}<1$). This scheme of separation would be feasible given there is a sufficient inertial force acting on both particles while the magnetic force acting on MPs is strong enough to overcome the sum of drag and inertial forces. Hence, it is important to optimize the operating conditions of the device so as to achieve co-existence of magnetic and inertial forces of appropriate magnitudes but opposite directions. These forces are dependent on parameters such as flow rate, channel aspect ratio and particle sizes (Eq. 1-3) under constant magnetic field conditions. A series of experiments were performed to ascertain the effect of these parameters on distribution of particles in our device. The findings were applied to discern optimum conditions for achieving two particle fractionation, with size similarity, in the MIMF device.

3.4.2 Effect of Flow Rate on Duplex MIMF

Experiments were performed with a mixture of 11 µm (10-13.9 µm) magnetic and 15 µm (10-19 µm) NMPs in the device with AR of 1.8 as discussed in the Materials and Methods section. There were a total of approximately 10^6 particles per mL of sample used in this study. We varied the input flow rate from 1 to 9 mL h^{-1} and captured distribution of particles in the expansion zone of the device (region B in Fig. 3). The experiments were firstly performed without any magnet to gauge the distribution of particles with respect to inertial and drag forces generated in the device as shown in Fig. 10a (i-iv). We observed that both particles were randomly distributed across the

width of the channel at lower flow rates (<6 mL h^{-1}, when the corresponding Re_p was 0.1–0.6 for both particles, Fig. 10a (i-ii)) which confirmed the absence of significant inertial forces in the device to focus the particles. However, particles started getting focused in the center of the channel at higher flow rates (>6 mL h^{-1}) as observed in Fig. 10a (iii-iv). In these cases, the inertial forces grew in magnitude and were able to dominate the distribution of particles as Re_p became greater than 0.7 for 11 µm MPs and greater than 1.3 for 15 µm NMPs.

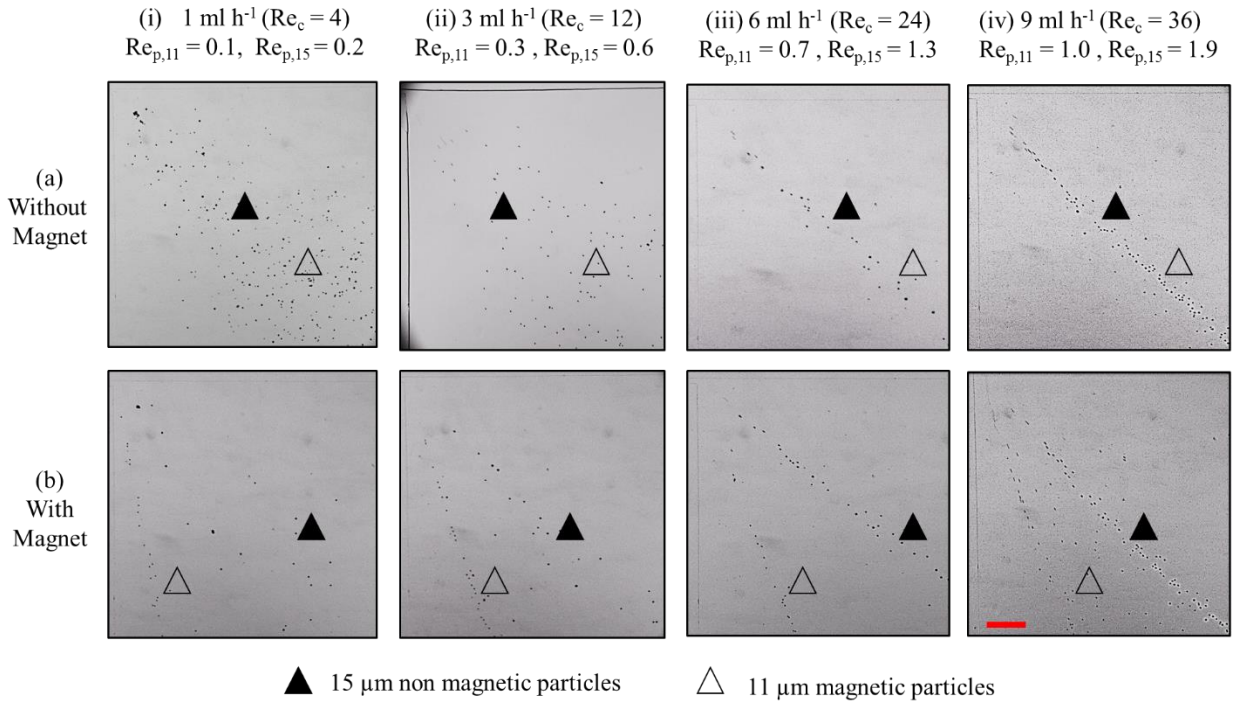

Figure 10. *Experimental observations of the effect of flow rate (1-9 mL h^{-1}) on behaviour of 11 µm magnetic and 15 µm NMPs in Region B of the MIMF device with AR of 1.8. a(i-iv) show the results without any magnet in the setup while b(i-iv) demonstrate the results at identical conditions but with presence of the permanent magnet in the setup. The flow direction was from left to right in all images and the scale bar corresponds to 250 µm.*

The above experiments were repeated under same operating conditions with a magnet in the setup. Observations of particles distribution is presented in Fig. 10b (i-iv). At all flow rates under 9 mL h^{-1}, the MPs were magnetically focused closer to the channel wall of the expansion zone as

$Re_{p,11}$<1 in all these cases (i.e. inertia less significant). The NMPs were found dispersed in the channel at flow rates less than 6 mL h^{-1} as described above, however they got strongly focused in the center at flow rates of more than 6 mL h^{-1} ($Re_{p,15}$=1.3 and higher). At a flow rate of 6 mL h^{-1}, it was found that both MPs and NMPs were focused in the device and completely separated from each other. Interestingly, at the flow rate of 9 mL h^{-1} (Re_c=36), we observed that 11 µm MPs were slightly defocused in the expansion channel while the 15 µm NMPs were still strongly focused. Accordingly, no separation was possible at this flow rate as the inertial forces started to become stronger ($Re_{p,11}$=1) than the magnetic forces and push the MPs towards the center of the channel. Hence, we concluded that particle manipulation was governed by magnetic focusing at flow rates <6 mL h^{-1} and by inertial focusing at flow rates >6 mL h^{-1} in this device (AR=1.8). In terms of particle Reynolds number, fractionation was stronger when Re_p was less than unity for 11 µm magnetic and more than unity for 15 µm NMPs (Fig. 10biii).

We also measured the exit position of particles at region C of the device with respect to the expansion zone baseline, using the method detailed in the Materials and Methods section. Fig. 11 shows the mean position and distribution of both 11 µm magnetic and 15 µm non-magnetic particles when experiments were performed with a magnet in the setup corresponding to observed distributions in Fig. 10b (i-iv). At low flow rates of 1 and 3 mL h^{-1}, the NMPs were dispersed over the regions 4.60±1.70 mm and 4.60±1.40 mm away from the baseline, respectively. However, the 11 µm MPs were focused over the regions 1.71±0.15 mm and 1.74±0.10 mm away from the baseline at the low flow rates of 1 and 3 mL h^{-1}, respectively. At 6 mL h^{-1}, the 11 µm MPs were still focused; however, they were found to be slightly shifted towards the center of the channel at 2.30±0.10 mm away from the baseline. The NMPs were also focused in the region 4.60±0.12 mm away from the baseline at 6 mL h^{-1} due to dominance of

inertial forces illustrated in Fig. 10. At 9 mL h^{-1}, the 11 µm MPs were slightly defocused due to excess inertial forces and distributed over region 2.70±0.80 mm away from the baseline while 15 µm NMPs were still focused at 4.60±0.10 mm away from the baseline.

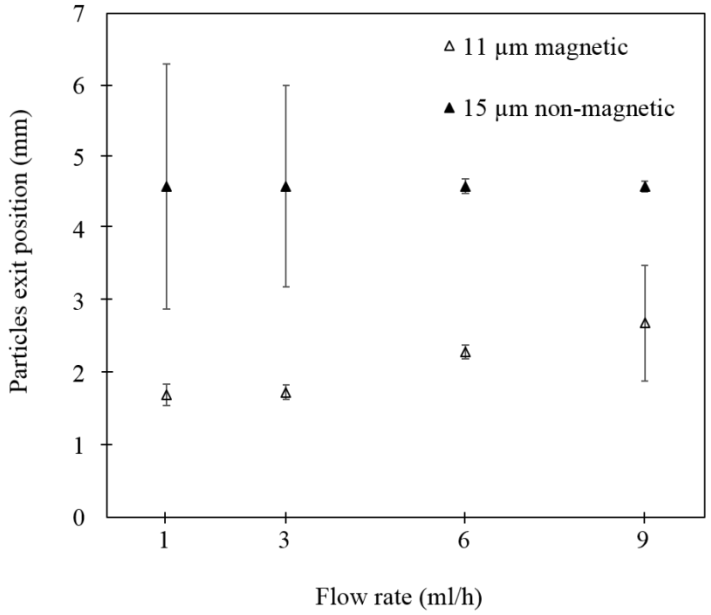

Figure 11. *Quantification of exit position (mean and standard deviation) of 11 µm magnetic and 15 µm NMPs in the MIMF device with AR of 1.8 when experiments were performed with a magnet at various flow rates. The exit positions were measured with respect to the baseline of the device.*

Essentially, inertial forces could be used as a means to differentiate NMPs from MPs in a sheathless fashion and without any need for HGMF elements like magnetic comb, needle or stripes [18,70,88]. However, we noticed that inertial forces grow in magnitude with increase in flow rate (Re_c) and eventually interfere with magnetic focusing of MPs. Hence, it is required that the device performance be characterized to achieve an optimal flow rate where inertial, drag and magnetic forces are of comparable magnitude. The intermediate flow rate regime of 6 mL h^{-1} (Re_c=24, Fig. 10 and 11) is the optimal choice for achieving fractionation of MPs from NMPs in the device with AR=1.8, as there is coexistence of inertial and magnetic focusing under this condition.

3.4.3 Effect of Channel Aspect Ratio on Duplex MIMF

The ratio of particle size to characteristic length of channel significantly affects the magnitude of inertial focusing forces exerted onto particles (Eq. 1). In this section, the effect of AR on the distribution of particles in the expansion zone of the device (regions B shown in Fig. 3) was investigated. Aspect ratios of 1.8, 2.25 and 3 were tested by fabricating devices with heights of 50, 40 and 30 µm, respectively. The experiments were performed with a mixture of 11 µm magnetic and 15 µm NMPs in the device at flow rates of 1, 3, 6 and 9 mL h^{-1} with a magnet in the setup. There were a total of approximately 10^6 particles per mL of sample used in this study. The results of observed distribution of particles in region B of the device are shown in Fig. 12.

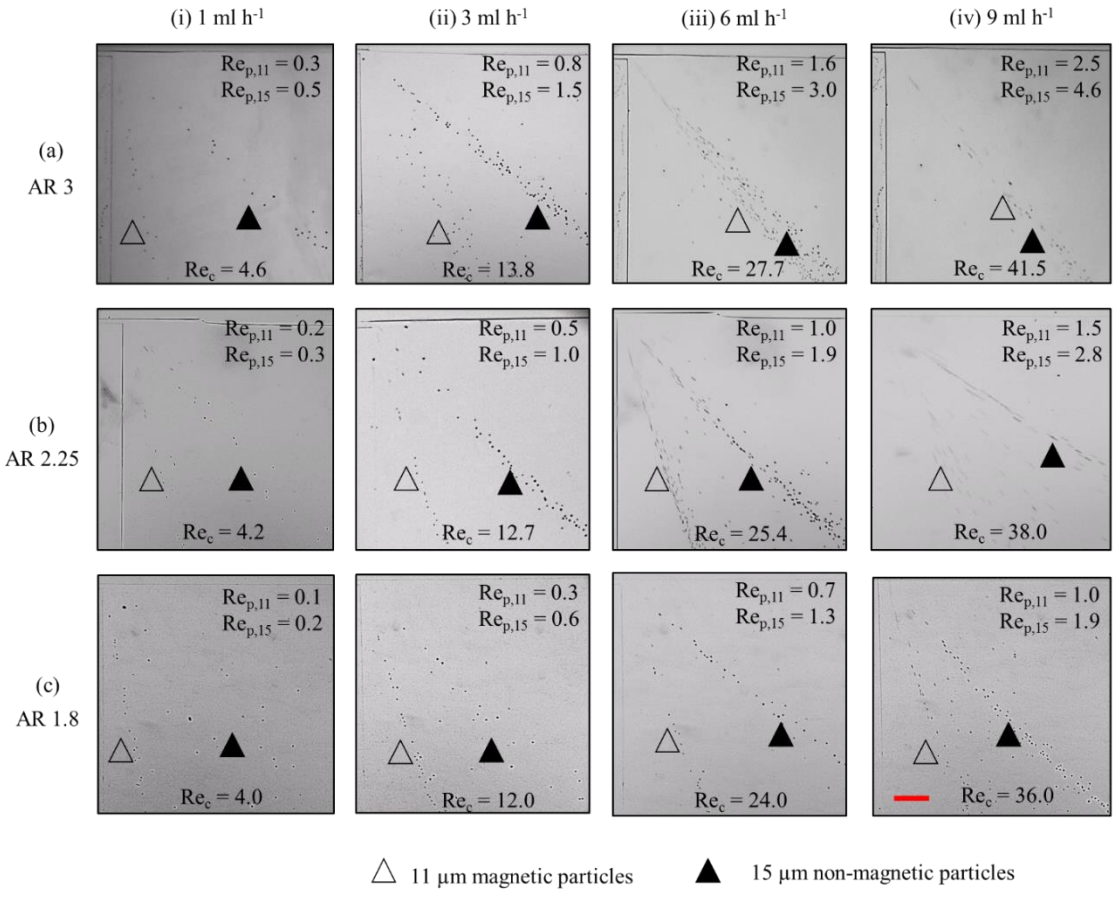

Figure 12. *Experimental observations of the effect of channel Aspect Ratio (AR=width/height) on behavior of 11 µm magnetic and 15 µm NMPs in Region B of the MIMF device at various flow rates*

(columns). Rows a, b and c correspond to experiments performed with device ARs of 3, 2.25 and 1.8, respectively. The flow direction was from left to right in all images and the scale bar corresponds to 250 μm.

As seen in Fig. 12, at a flow rate of 1 mL h^{-1}, the change in AR from 1.8 to 3 led to enhancement of inertial focusing of NMPs owing to increase in particle Reynolds number ($Re_{p,15}$) from 0.2 to 0.5. We found that 15 μm NMPs were focused in the center of the device with AR of 3 and 2.25, however they were found to be randomly distributed in the device with AR of 1.8. The 11 μm MPs were found to be focused magnetically close to the sidewall in all three devices at this low flow rate. $Re_{p,11}$ increased from 0.1 in device with AR=1.8 to 0.3 when AR=3, at which inertial focusing is not very strong allowing the 11 μm MPs to be under the dominant effect of magnetic forces. At a flow rate of 3 mL h^{-1}, it was observed that 15 μm NMPs were still defocused in the device with AR of 1.8 ($Re_{p,15}$=0.6), but focused in the other two devices ($Re_{p,15}$=0.9 for AR=2.25 and $Re_{p,15}$=1.5 for AR=3). The 11 μm MPs, however, were found to be slightly defocused from the wall (due to inertia) in the device with AR of 3 ($Re_{p,11}$=0.8) but still well-focused magnetically at the wall in the devices with AR of 2.25 ($Re_{p,11}$=0.5) and 1.8 ($Re_{p,11}$=0.3) at a flow rate of 3 mL h^{-1}. It is worth noting that fractionation of MPs from NMPs in the device with AR of 3 was not possible at any flow rate higher than 3 mL h^{-1}. At a flow rate of 6 mL h^{-1}, we found that both magnetic and non-magnetic particles were separately focused in the device with AR of 2.25 ($Re_{p,11}$=1.0 and $Re_{p,15}$=1.9) and 1.8 ($Re_{p,11}$=0.7 and $Re_{p,15}$=1.3) with some inertial defocusing of MPs in the device with AR of 2.25 due to the high $Re_{p,11}$=1.0. Fractionation of MPs from NMPs was not possible efficiently in any of the devices at a flow rate of 9 mL h^{-1} ($Re_{p,11}$ = 2.6, $Re_{p,15}$ = 4.6 for AR = 3; $Re_{p,11}$ = 1.5, $Re_{p,15}$ = 2.8 for AR = 2.25; and $Re_{p,11}$ = 1.0, $Re_{p,15}$ = 1.9 for AR = 1.8) because MPs were either inertially focused and mixed with non-

magnetic ones in the center (AR=3) or dispersed in the channel due to comparative strength of inertial forces with magnetic forces (AR=1.8 and 2.25).

The results in Fig. 13 fully support our claim of the need for interaction between comparable inertial and magnetic forces to achieve efficient fractionation in our device. Overall, we observed that with the decrease of AR (i.e., increase of channel height), inertial forces acting on both particles decreased at a given flow rate (due to drop in the axial velocity), which in turn allowed the magnetic forces to become comparatively dominant on 11 µm MPs to pull them away from the stream of 15 µm NMPs. Accordingly, distinct separation of the two particle streams could be obtained at higher flow rates when AR of the MIMF device was reduced. The observation pertaining to insufficient separation in the device with AR of 3 at any flow rate greater than 3 mL h^{-1} ($Re_{p,11} > 1.7$ and $Re_{p,15} > 3.0$) can be attributed to dominance of inertial forces at high flow velocities over magnetic forces as explained by Eq. 1 and Eq. 3.

Positional distribution of 11 µm MPs and 15 µm NMPs at 6 mL h^{-1} flow rate (Figs. 13iii) was quantified in region C of the device (Fig. 3), assuming baseline as the reference and results are presented in Fig. 13. It was found that 15 µm NMPs were concentrated in the region 4.60±0.10 mm away from the baseline in all three devices. However, the 11 µm MPs were concentrated at 1.70±0.10 mm, 2.20±0.3 mm and 4.30±0.1 mm away from the baseline in the devices with AR of 1.8, 2.25 and 3 respectively. This quantitative result also demonstrate the shifting of MPs from the sidewall towards the center of the channel as the AR is increased, confirming that inertial forces become more dominant on all particles as the height of the channel decreases from 50µm to 30µm.

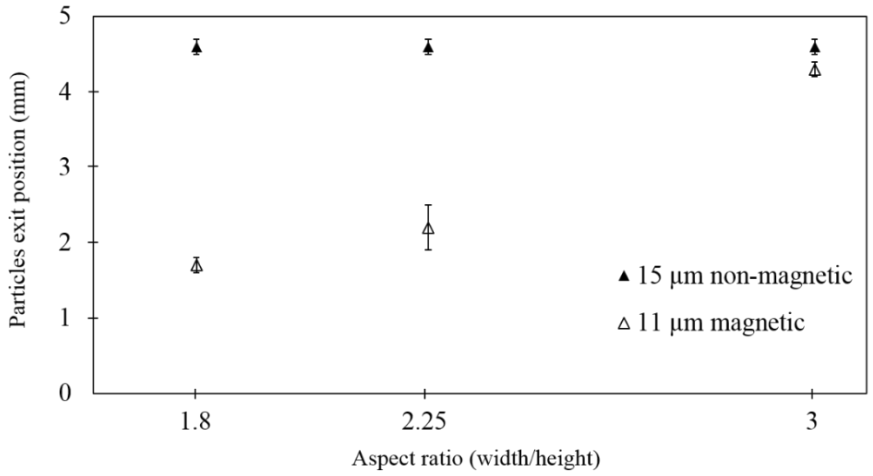

Figure 13. *Quantification of exit position (mean and standard deviation) of 11 µm MPs and 15 µm NMPs in MIMF devices with ARs of 1.8, 2.25 and 3, at a flow rate of 6 mL h^{-1}. The exit positions were measured with respect to the baseline of the device.*

In a nutshell, the investigation into aspect ratio of devices led to two important conclusions. Firstly, the distribution of particles greatly varies with change in AR of the device and hence the device design must be done carefully to achieve the desired results. Especially, the separation scheme is more feasible when the particle Reynolds number for 11 µm magnetic particle ($Re_{p,11}$) is less than 1. Secondly, Fig. 12 clearly shows that it is possible to improve the throughput of fractionation from 1 mL h^{-1} to 6 mL h^{-1} just by adjusting the AR from 3 to 1.8. This better understanding of behavior of particles with respect to AR of the channel enabled development of MIMF devices with throughputs higher than 6 mL h^{-1} for fractionation of two to four particles in the rest of the chapter.

3.4.4 Effect of Size of Magnetic Particles on Duplex MIMF

The magnitude of inertial forces, as seen in Eq. 1, is strongly affected by size of particles [12,74]. Herein, we performed the duplex fractionation experiments with MPs of diameter 5, 11, or 35 µm mixed one at a time with 15 µm NMPs to elucidate the effect of size on the dynamic

competition between inertial and magnetic forces. We chose these sizes to ensure that the device principle can be applied for fractionating a wide range of targets from a mixture. The experiments in previous section indicated that the device throughput can be improved by decreasing the AR of the channel. Hence, we chose to perform this set of experiments in a MIMF device with AR of 1.5 to achieve fractionation at a higher flow rate of 9 mL h^{-1} that was not achievable with the previous devices. Fig. 14 shows the distribution of the abovementioned pairs of particles after fractionation in the channel at region C of the device.

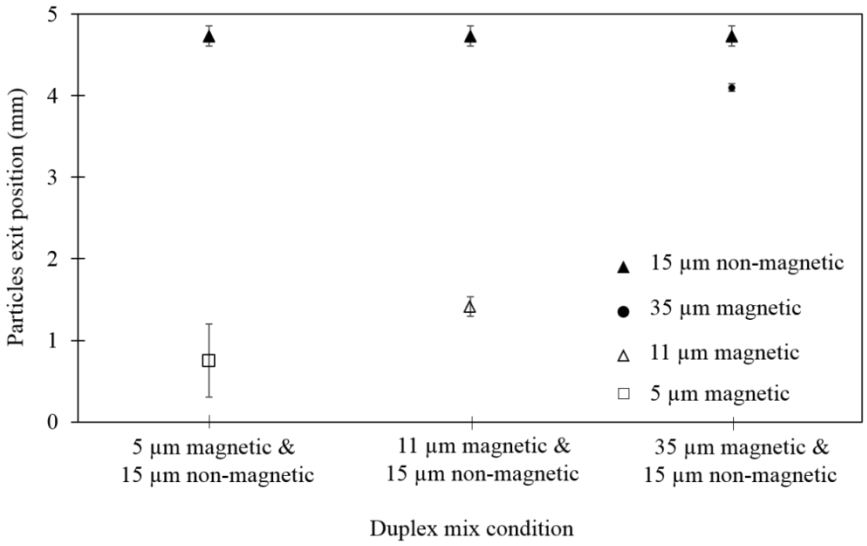

Figure 14. *Quantification of exit position (mean and standard deviation) of various sizes (5, 11 or 35 µm) of MPs sorted from 15 µm NMPs in a duplex MIMF devices with AR of 1.5 at a flow rate of 9 mL h^{-1}. The exit positions were measured with respect to the baseline of the device.*

In the experiments conducted with a mixture of 5 µm magnetic and 15 µm non-magnetic particles, it was found that NMPs were focused close to the center of the channel, 4.70±0.12 mm away from the baseline, because of dominant inertial forces at 9 mL h^{-1} flow rate ($Re_{p,15}$=1.4). The 5 µm MPs were found to be distributed at 0.64±0.34 mm and completely fractionated from the NMPs ($Re_{p,5}$=0.2, hence no inertial focusing). The experiments were performed at a

concentration of approximately 10^8 particles per mL of water (mixture of ~10^8 MPs and ~10^5 NMPs per mL), which resulted in an unprecedented high throughput of 10^9 particles per hour.

In the experiments performed with a mixture of 11 µm magnetic and 15 µm non-magnetic particles, the MPs ($Re_{p,11}$=0.8, weaker inertial forces overpowered by magnetic forces) were magnetically focused in the region around 1.41±0.12 mm away from the baseline while NMPs were found inertially focused close to the center as before. This fractionation study was performed at a throughput of 10^7 particles per hour as the concentration of particles used for experiments was about 10^6 particles per mL of water (mixture of ~10^6 per mL (due to lower concentration of original batch) magnetic and ~10^5 per mL NMPs).

When 35 µm MPs were tested in mixture with 15 µm NMPs, they were found distributed over the region 4.10±0.04 mm away from the baseline ($Re_{p,35}$=7.8). Since $Re_{p,35}$ was much greater than 1, these particles experienced more significant inertial forces than the 5 µm and 11 µm MPs in previous experiments, and were focused closer to the center of the channel. However, magnetic forces were still able to pull them away from the stream of NMPs focused purely by inertia at the center of the channel. The throughput of these experiments was about 10^6 particles per hour as the study was conducted at a concentration of about 10^5 particles per mL (mixture of ~10^4 per mL magnetic and ~10^5 per mL NMPs).

We observed that there was a complete fractionation of each type of MPs from NMPs in all three experiments described above. Moreover, quantification of positions of particles in the device led to a finding that the larger the MPs were, the closer they became to the stream of 15 µm NMPs in the center of the channel. This can be explained by the magnitude of inertial forces that increases more rapidly with particle diameter (4^{th} power dependence in Eq. 1) as compared to magnetic forces (3^{rd} power dependence in Eq. 3). Accordingly, interaction between magnetic and sum of

inertial and drag forces can easily be used as a scheme to achieve multiplex particle fractionation with MIMF method. This has been pursued in the next two sub-sections of this chapter.

3.4.5 Triplex MIMF

In this section, we investigated simultaneous fractionation of three MPs of sizes 5, 11 and 35 µm with MIMF. As we observed in the previous section, cumulative effect of magnetic, drag and inertial forces leads to size-dependent ordering of MPs in the device, hence offering a scheme to perform multi-particle fractionation in an inertio-magnetic device. Experiments were performed in a MIMF device with AR of 1.5 at a flow rate of 9 mL h^{-1}. This study was conducted at a total concentration of approximately 10^6 particles per mL. Particle distribution images were captured at region B of the device with and without the magnet in the setup and results are presented in Fig. 15.

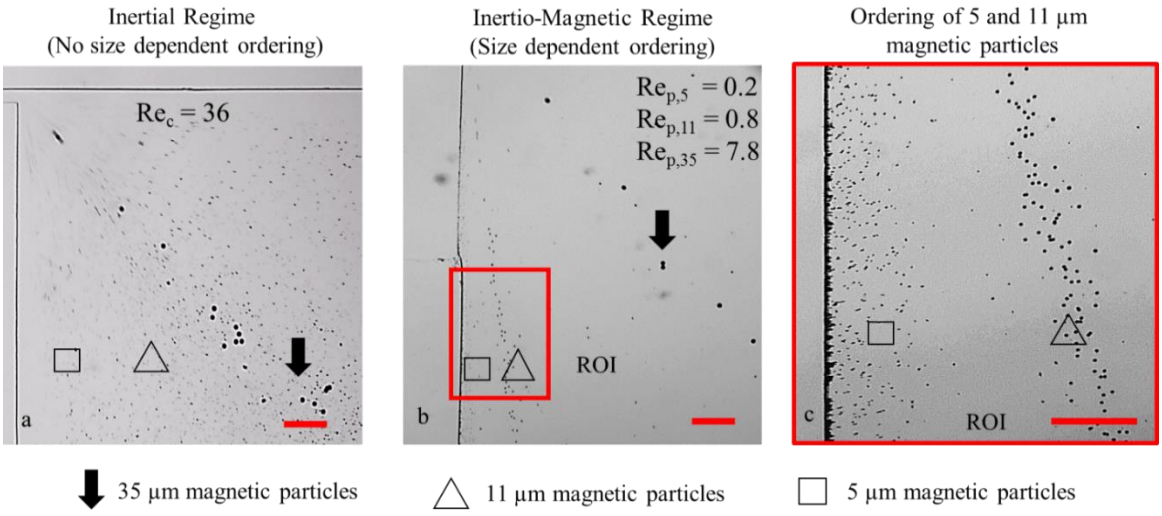

Figure 15. *Experimental observations (at region B of the device) showing separation of 5, 11 and 35 µm MPs in a MIMF device with AR=1.5 at 9 mL h^{-1} flow rate. Distribution of all three particles is demonstrated (a) without any magnet and (b-c) with a magnet in the setup. The magnified view of 5 and 11 µm MPs corresponding to the region of Interest (ROI) in (b) is shown in (c). The flow direction was from left to right in all images and scale bars correspond to 250 µm.*

Firstly, a mixture of all three particles was injected into device and their distribution was monitored in region B without any magnet in the setup. Fig.15a shows that all particles were randomly distributed in the device in the absence of any magnetic force. We observed that 35 µm MPs were focused in the center of the channel, indicating the presence of a significant inertial force on these particles ($Re_{p,35}$=7.8). However, it was difficult to discern the distribution of 5 and 11 µm MPs distinguishably in this condition ($Re_{p,5}$=0.2 and $Re_{p,11}$=0.8). Then, we performed the same experiment involving all three particles but with a magnet in the setup and the particle distribution results are presented in Fig. 15b and 15c. It was found that 35 µm MPs were still focused very close to the center of the channel, indicating that there was a dominance of inertial forces on these particles as discussed in the previous section and Fig. 14. Inertial forces overpowered the sum of drag and magnetic forces on 35 µm MPs and did not allow them to be attracted much towards the magnet in the device. On the other hand, we found that 5 and 11 µm MPs were more strongly attracted by the magnet and were focused much closer to the wall of the channel as compared to 35 µm MPs. The streams of 5 and 11 µm MPs were not clearly visible in Fig. 15b and hence we captured their distribution at a higher magnification as shown in Fig. 15c. These particles were found to be completely separated from each other and, as expected, the 5 µm MPs were closer to the wall than 11 µm MPs. Accordingly, we experimentally verified that the smaller the MPs, the closer their positions are to the wall in a MIMF setup. We emphasize that existence of one type of force in the device will either lead to no fractionation at all (with inertial forces only) or potentially fractionation at a significantly lower throughput and efficiency (with magnetic forces only) based on our previously reported method [92]. As demonstrated in this section, it is the proper design of the device geometries and the co-existence of inertial and

magnetic forces at high flow rates that led to accomplishment of triplex fractionation at high throughputs with the MIMF method.

3.4.6 Fourplex MIMF

Here, we used the MIMF technique to achieve fractionation of three MPs and a NMP. The experiments were performed with mixtures of 5, 11 and 35 µm MPs and 15 µm NMPs in water at a total concentration of about 10^6 particles per mL. The samples were injected into the MIMF device with AR of 1.5 at a flow rate of 9 mL h^{-1} (Re_p = 0.2, 0.8 and 7.8 for 5, 11 and 35 µm MPs respectively and Re_p=1.4 for NMPs) and images were captured at region C of the device (Fig. 16a) for quantifying particles' exit positions with respect to the expansion zone baseline (Fig. 16b). We could not capture the entire spectrum of four fractionated particles in one frame at the downstream region of the device due to the limited field of view of our microscope, as particle bands were distributed over a distance of about 5 mm across the width of the channel. Hence we captured the position of 15 µm non-magnetic and 35 µm magnetic particles in one frame at upper half of region C of the device closer to the center, and 5 and 11 µm MPs in the other frame at lower half of region C closer to the wall.

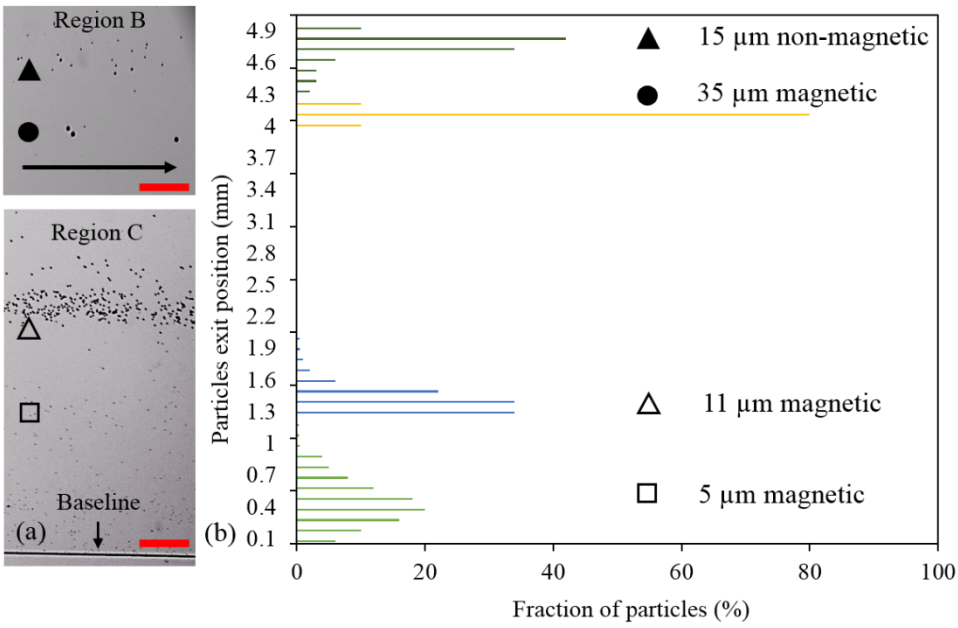

Figure 16. *Fourplex MIMF. (a) Experimental observations (at region C of the device) of simultaneous sorting of four particles (5, 11 and 35 µm MPs and 15 µm NMPs) in a MIMF device with AR=1.5 at 9 mL* h^{-1} *flow rate. Due to limited field of view of our microscope, we captured the images in two halves at region C, to exhibit sorting of all four particles in the device. The flow direction was from left to right in both images and scale bar corresponds to 250 µm. The flow direction is from left to right as indicated by arrow. (b) Quantification of exit positions and fractions of 5, 11 and 35 µm MPs and 15 µm NMPs sorted in the MIMF device. The exit positions were measured with respect to the baseline of the device.*

As expected, the 15 µm NMPs were inertially focused in the center and the 35 µm MPs were found close to the stream of NMPs as they were strongly under the effect of inertial forces owing to their large sizes (see previous section). Magnetic forces dominated the focusing of 5 and 11 µm MPs in region C of the device and they were both focused closer to the wall and arranged in a sequence similar to what was observed in the triplex MIMF (i.e., smaller particles closer to the wall due to less dominant inertial forces).

Further, we quantified the distributed positions of all particles with respect to the baseline in the device (Fig. 16b), using the method described before. The 15 µm NMPs were found concentrated in the region 4.70±0.12 mm away from the baseline and 35 µm MPs were focused at 4.10±0.04

mm. Both of these particles were under the dominant influence of inertial focusing forces while magnetic forces separated the MPs from the non-magnetic ones. The 11 µm MPs were found closer to the wall and at 1.41±0.12 mm away from the baseline while 5 µm MPs were found at 0.49±0.22 mm, both under the dominant effect of magnetic forces while taking advantage of inertial competing forces to get separated from each other.

The position of fractionated particles has been provided as guideline here and these particles can easily be collected separately by implementing outlets based on the calculated exit positions of these particles presented in Fig. 16. This was outside the scope of this research and will be pursued in the future for sorting of microorganisms based on MIMF method. It should be highlighted that, for this particular MIMF design and flow rate condition, the largest MPs that could be separated from NMPs in our device were 35 µm in diameter. Any further increase in the size of MPs could led to their mixing with the NMPs. Accordingly, it should be noted that although the MIMF method is strong in multiplex fractionation based on competition between magnetic, inertial and drag forces, but it has its own limitations in terms of the size of particles that can be handled with this device. We anticipate that our proof-of-principle results will pave the way for further investigation of this hybrid method to develop custom-designed MIMF devices based on end user needs with respect to number and size of particles, throughput, and fractionation efficiency.

3.5 Conclusions

We have presented a novel MIMF method for fractionation of up to four magnetic and non-magnetic microparticles in an inertio-magnetic microfluidic device, which addresses several drawbacks of currently available magnetic fractionation methods such as low throughput, requirement of sheath flow, inability to fractionate multiple targets simultaneously and

complicacies in fabricating special HGMF elements such as magnetic combs, stripes or needles. We have shown that magnetic forces interact with and complement drag and inertial forces synergistically in a straight microchannel to exhibit strong size-dependent ordering of magnetic and NMPs, hence paving the way for their fractionation at a downstream hydrodynamic expansion zone. We showed that fractionation of similar-size MPs and NMPs in MIMF devices could be achieved efficiently at a throughput as high as 10^9 particles per hour. We identified several dominant factors governing behavior of particles in the device and conducted experiments to elucidate their effects on fractionation performance. Further, the insights gained from these parametric studies were applied to achieve simultaneous fractionation of four particles (5, 11 and 35 µm magnetic and 15 µm NMPs) for the first time in a straight microfluidic device using inertial focusing and magnetophoresis. We envision that the MIMF technique would enable easy handling of complex and dense mixture of particles in a wide variety of applications. The technique has a great potential for use in affinity-based immunomagnetic tagging, extraction and sorting of multiple cells and microorganisms in water and body fluids.

Chapter Four

4 Sheathless and Multiplexed Magnetophoretic Sorting of Magnetic and Non-Magnetic Microparticles in Non-Newtonian Fluids[‡]

4.1 Introduction

Sorting operation has multifarious applications in biotechnology [98], medicine [99] and diagnostics [100]. Many techniques such as dielectrophoresis [101], acoustic [102], deterministic lateral displacement [103], pinched flow fractionation [104] and inertial microfluidic [105] have been developed to achieve separation at micro-scale. However, microfluidic-based magnetophoretic sorting technique is preferred to handle complex mixtures of micron-sized entities such as micro-particles and cells [80,106,107] as many parameters including fluid properties do not have any significant influence on the magnetic field. Several magnetic sorting microdevices have been proposed in the literature such as free flow magnetophoretic size-based sorting of magnetic microparticles [14], electromagnetic manipulation of single magnetic beads [108], multi-target magnetic activated cell separation [18], magnetophoresis integrated hydrodynamic filtration [43] and a recently-introduced inertia-magneto-hydrodynamic fractionation technique (in chapter 2 and 3) by us [92]. Majority of these magnetic techniques have demonstrated sorting of biological and non-biological targets solely in Newtonian fluids

[‡] This chapter will be submitted in whole as a manuscript for publication in *Applied Physics Letters*.

like water. However, the biological fluids in which target sorting has to be achieved for diagnostic purposes are mostly non-Newtonian such as undiluted blood and saliva [109,110].

The particles suspended in non-Newtonian fluids behave differently in comparison to their behavior in Newtonian fluids because of experiencing elastic lift forces that become dominant in such fluids [111]. For instance, 1.9 μm microparticles in a square 20×20 μm^2 microchannel occupy multiple equilibrium positions when the medium is a Newtonian fluid [76], while 10 μm microparticles focus only in the center of a 100×100 μm^2 channel when suspended in a non-Newtonian viscoelastic solution of 8% polyvinylpyrrolidone [111]. Clearly, there is a need to enumerate the behavior of MPs and NMPs under the effects of elastic and magnetic forces for achieving their separation when suspended in non-Newtonian fluids as the knowledge of magnetophoretic separation in Newtonian fluids is not directly applicable here. Giudice et al. [90] recently reported a microfluidic device for separating a magnetic particle from a non-magnetic particle suspended in a viscoelastic solution of polyacrylamide (PAM). However, their technique required an external buffer sheath flow and could only achieve separation of two particles at a time.

In this chapter, we investigated the applicability of our sheath-less fractionation technique [92] in triplex separation of MPs and NMPs in a non-Newtonian polyethylene oxide (PEO) fluid. The effect of flow rate and viscosity (i.e., PEO concentration in water) on fractionation of particles suspended in this surrogate non-Newtonian fluid was studied to achieve triplex sorting of microparticles without any external sheath buffer. The parametric study helped to identify the optimal operating conditions required for achieving multi-particle magnetophoretic sorting in non-Newtonian fluids for the first time.

4.2 Methods and Materials

4.2.1 Materials

We performed experiments with a mixture of 5 μm and 11 μm diameter MPs (Spherotech Inc., USA) and 15 μm diameter NMPs (Phosphorex Inc., USA) suspended in non-Newtonian fluids prepared by mixing PEO powder (Molecular Weight ~ $2x10^6$ Da, Sigma Aldrich USA) in water at different concentrations (500, 1000, and 2000 ppm). These concentrations correspond to zero shear viscosities of 1.8, 2.3 and 4.1 mPa.s, respectively [112]. The total concentration of all three particles used for experimentation was 10^6 particles per mL. We added about 0.5% (v/v) of Tween 20 (Sigma Aldrich) to keep particles dispersed in PEO solution.

4.2.2 Device Design, Fabrication and Experimental Procedures

The device design has been presented in Fig. 3, however the width of focusing zone was 70 μm and height of the channels were 65 μm. A cuboid magnet ($20\times10\times5$ mm^3, Indigo Instruments, Canada) was placed by the side of focusing zone. The device master mold was fabricated using standard photolithography and the device was prepared in PDMS using soft lithography as reported earlier [92]. The experiments were performed by injecting particles suspended in PEO-water solutions into the device at desired flow rates (0.1–1 mL h^{-1}) using a syringe pump (KD Scientific, USA). Images and videos of fractionated particles were captured using a 162 fps camera (Point Grey, BC, Canada) mounted on an inverted microscope (Bioimager, ON, Canada). We used the freeware ImageJ for quantifying the distribution of particles in captured images as described in chapters 2 and 3.

4.3 Working Principle

The forces acting on MPs and NMPs in a non-Newtonian fluid in our device are discussed in this section. All particles experience elastic lift forces towards the center of the channel (Eq. 4).

$$F_{EL} \sim \lambda(a/w)^3 Q^3, \quad (4)$$

where λ is relaxation time (ms), w is width of channel (m) and Q is flow rate (m^3/s) [111–113]. The strength of elastic forces is characterized by the Weissenberg Number ($Wi=2\lambda Q/w^2h$) [111,114].

The particles also experience net inertial lift forces (F_{IL}) expressed as sum of wall and shear induced lift forces (Eq. 1) [45,46]. The magnitude of inertial lift forces on a particle is indicated by the particle Reynolds number (Re_p). It has been reported that for $Re_p \geq 1$, the inertial forces are dominant in a system as fully demonstrated in chapter 3 [45]. However, we found that the Re_p for the particles in our device was less than 0.08, indicating that the inertial forces acting on particles were negligible. The magnitudes of drag (F_D) and magnetic (F_M) forces experienced by particles have been presented in Eq. 2 and Eq. 3.

4.4 Results and Discussion

In this section, we investigated the effect of flow rate and PEO concentration on fractionation of magnetic and non-magnetic microparticles in our device.

4.4.1 Effect of Flow Rate on Triplex Fractionation

Fig. 17 shows the effect of flow rate on fractionation of 5 µm and 11µm MPs and 15 µm NMPs suspended in 1000 ppm PEO using our microfluidic device. The experiments were first conducted without any magnet in the setup and images were captured at the entrance of expansion zone (Fig. 17a(i-v)). At a lower flow rate of 0.1 mL h^{-1} (Re=0.18, Wi=1.19), all three

particles were found to be focused on a single stream as seen in Fig. 17a(i). Similar observation of particles focusing in the center of a square microchannel has been reported in the literature [111]. We noticed a transition from focusing on a single line to focusing on multiple streams as the flow rate was increased to 0.75 mL h^{-1} (Re=1.34, Wi=8.90) in Fig. 17a(iv). This behavior can be attributed to increase in magnitude of elastic lift forces with increase in flow rate. These elastic lift forces promote focusing of particles in the center and four corners of the microchannel (at intersection of walls) where strain rate is minimum [114].

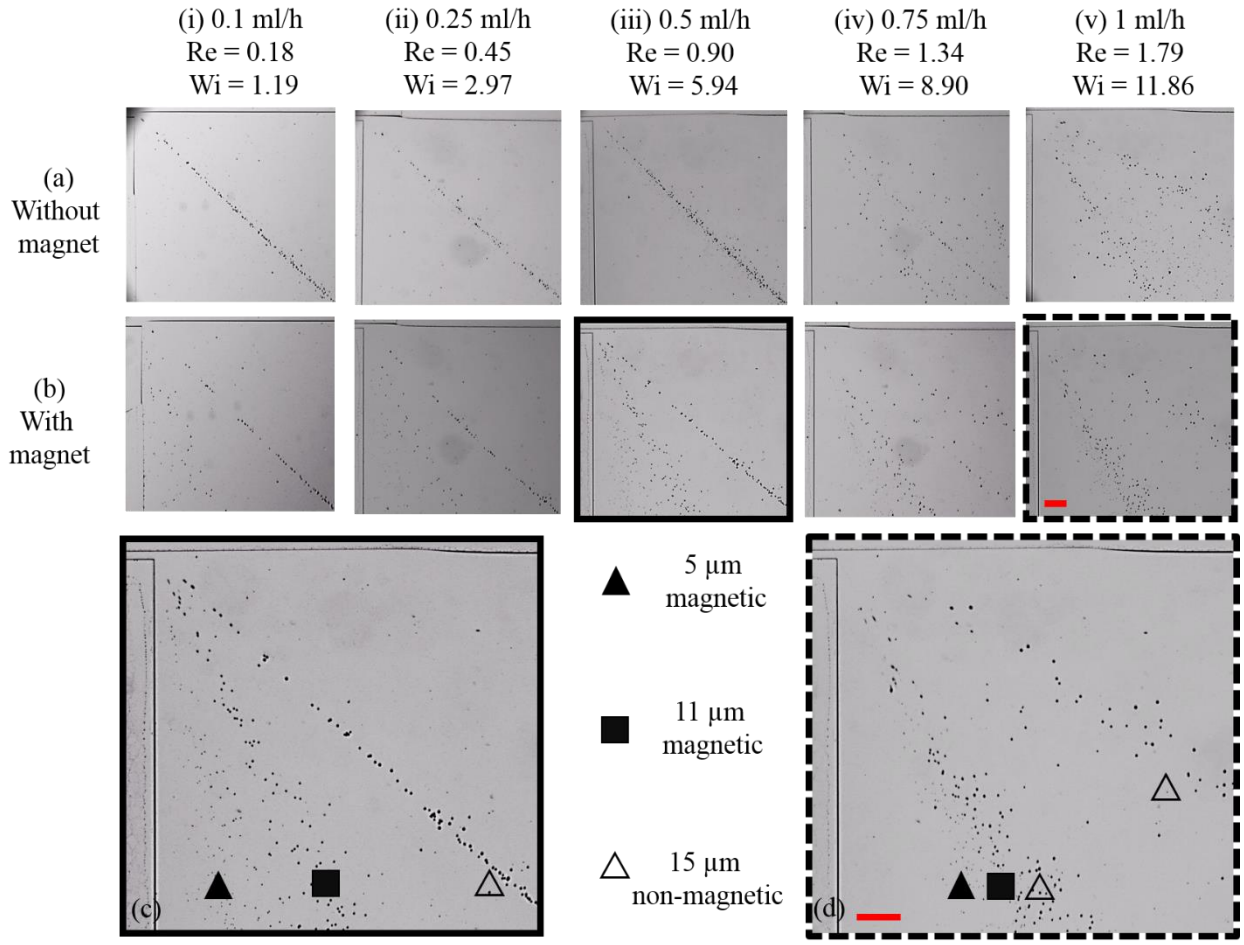

Figure 17. *Effect of flow rate (0.1–1 mL h^{-1}) on triplex fractionation performance of the device. Distribution of 5µm MPs, 11µm MPs and 15µm NMPs suspended in 1000 ppm PEO-water solution is demonstrated at the entrance of expansion zone (Region B of Fig. 3) when experiments were conducted a(i-v) without any magnet and b(i-v) with a magnet at equivalent conditions. (c) Magnified image of*

distribution of particles observed in b(iii). (d) Magnified image of distribution of particles observed in b(v). The flow direction was from left to right in all images and scale bar corresponds to 350µm.

We repeated the experiments presented in Fig. 17a with a magnet in the setup and corresponding distribution of particles is shown in Fig. 17b. As expected, the distribution of 15 µm NMPs remained the same as their motion was not influenced by magnetic forces. The 5 µm and 11 µm MPs, however, were attracted towards the sidewall due to the magnetic forces (Fig. 17b(i-iii)). The 11 µm MPs were found to be closer to the center than 5 µm MPs in the device. Hypothetically, the 5 µm and 11 µm MPs were magnetically focused on the wall in the focusing region and eventually separated from each other in the expansion zone (Fig. 3) hydrodynamically just like PFF. We also anticipate that the separation of 5 µm MPs from 11 µm MPs is enhanced (compared to conventional PFF) as 11 µm MPs shift towards the center in the focusing region due to elastic lift forces. We believe the shift of 11 µm MPs towards the center is greater than that of 5 µm particles because of strong size dependence of elastic forces (Eq. 4). A magnified view of the observed separation of particles corresponding to Fig. 17b(iii) is shown in Fig. 17c. The three distinct streams show 5 µm MPs closest to the wall, 15 µm NMPs in the center and 11 µm MPs positioned in between. We confirmed the distribution and position of particles by performing the same exact experiments with only one particle type at the time in the device. At any flow rate more than 0.75 mL h^{-1}(Re≥1.34, Wi≥8.90), we were unable to achieve any separation as observed in Fig. 17b(iv-v) because of presence of multiple focusing positions for NMPs as explained before. It was found that the streams of 5 µm and 11 µm MPs and 15 µm NMPs were mixed with each other towards the lower channel wall, and there was another stream of 15µm NMPs located towards the upper channel wall (Fig. 17d). Hence we concluded that the single line focusing of NMPs is compulsory for achieving sorting in our device.

4.4.2 Effect of PEO Concentration on Triplex Fractionation

Here, we investigated the effect of PEO concentration on fractionation performance of our device, as the magnitude of elastic lift forces increases with an increase in relaxation time of polymer solution. We prepared three different solutions having PEO concentrations of 500, 1000 and 2000 ppm in water with corresponding relaxation times of 4.3, 6.8 and 10.6 ms [112]. Fig. 18 shows the distribution of particles in the entrance to expansion zone of the device when experiments were performed with a magnet in the setup. At a flow rate of 0.25 mL h^{-1}, the 15 μm NMPs were found focused at the center of the channel at all three PEO concentrations. The MPs were fractionated closer to the wall at 500 ppm PEO concentration and separated from the stream of 15 μm NMPs. At a flow rate of 0.5 mL h^{-1}, we observed that 15μm NMPs were focused at the center at 500 and 1000ppm PEO concentrations, however they started to occupy multiple positions at 2000 ppm PEO as seen in Fig. 18ii(a-c). Fractionation of all three particles was observed in 500 and 1000 ppm PEO solutions, however multi-stream focusing of NMPs at 2000 ppm did not allow any fractionation. Further, we observed that particles tend to focus at multiple positions (Fig. 18iii(b-c)) at 1000 and 2000 ppm PEO concentrations at a flow rate of 0.75 mL h^{-1} and consequently no separation was possible. At this flow rate, the separation of all three particles was only possible in 500 ppm PEO solution. The focusing of NMPs in multiple positions directly depends on PEO concentration in water. The observation presented in Fig. 18c(i-iii) that multiple focusing occurs at lower flow rate in higher PEO concentration can be explained by the fact Wi increases with increase in relaxation time, which is 10.6 ms for 2000ppm PEO compared to 4.3 ms for 500ppm PEO. In conclusion we noticed that fractionation is possible at all PEO concentrations, however operating flow rate has to be lowered to achieve separation at higher PEO concentrations.

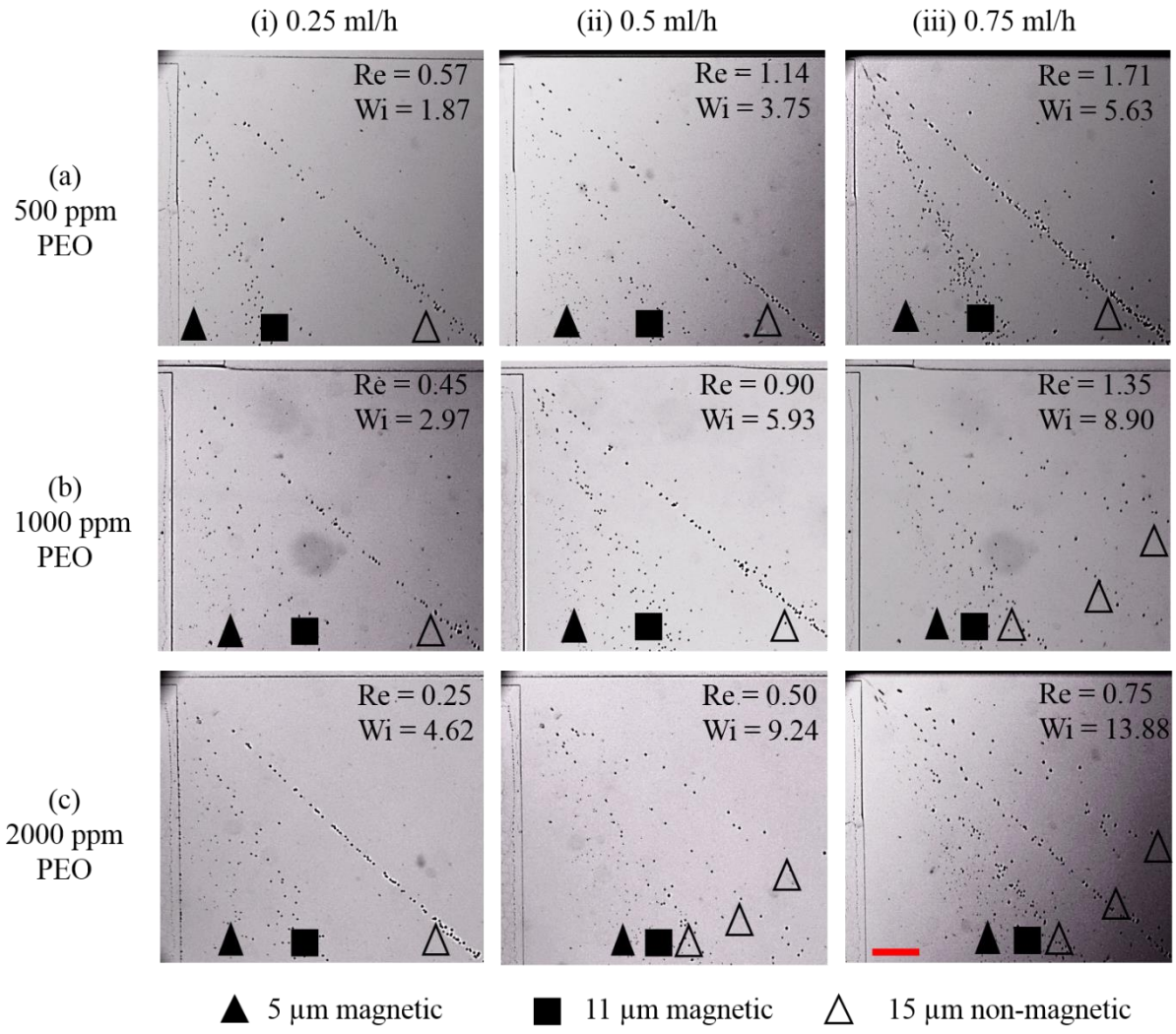

Figure 18. *Effect of PEO concentration (500, 1000, and 2000 ppm in water) on triplex fractionation performance of the device. Distribution of 5µm MPs, 11µm MPs and 15µm NMPs dispersed in a(i-iii) 500 ppm, b(i-iii) 1000 ppm and c(i-iii) 2000 ppm PEO solutions are demonstrated at different flow rates at the entrance of expansion zone (region B of Fig. 3). The flow direction was from left to right in all images and scale bar corresponds to 350µm.*

4.4.3 Triplex Sorting Characterization

After obtaining a sound understanding of fractionation of particles in our device at various flow rates and PEO concentrations, n=32 outlets were integrated across the width of the expansion zone to quantify the position of particles as they get sorted out from the device. The results in Fig. 19a correspond to a representative experiment performed with all three particles at a flow

rate of 0.5 mL h^{-1} in 1000 ppm PEO solution (Fig. 18b(ii)). We captured magnified images of the sorted particles in 5 outlets in each frame (examples shown in Fig. 19c and 19d) and counted the number of particles in these images using "Analyze Particles" function of the freeware ImageJ. We obtained the fraction of particles in each outlet by calculating the ratio of number of particles passing through each outlet to the total number of same particles passing through all outlets. The 5 μm MPs were expectedly found closer to the wall and mostly flowing through outlets 2-6 as observed in Fig. 19b. As we have discussed above in section 4.1.3, the 11 μm MPs were positioned closer to the center of the channel compared to the 5μm MPs. The 11 μm MPs were mostly distributed to outlets 6-11. The 15 μm NMPs, unperturbed by magnetic forces, were focused close to the center of the channel and found at outlets 14-16 of the device.

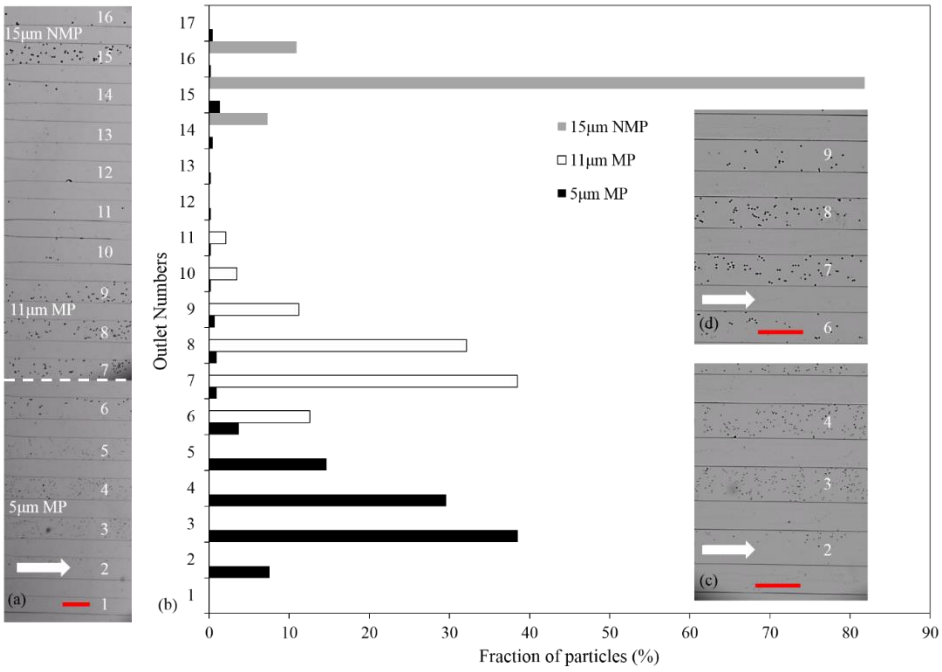

Figure 19. *Sorting characterization of 5μm MPs, 11μm MPs and 15μm NMPs in 1000ppm PEO in outlets of the device at a flow rate of 0.5 mL h^{-1}. (a) Distribution of particles in different outlets constructed by combining two images at the junction of outlets 6 and 7 as shown by the dashed line. (b) Quantification of exit position of sorted particles showing the fraction of different particles passing through the outlets of the device. (c) Magnified view of the sorted 5μm MPs passing through outlets 1-5.*

(d) Magnified view of the sorted 5μm and 11μm MPs passing through outlets 6-9. The flow direction was from left to right as shown by arrows. The scale bars correspond to 350μm.

As observed in Fig. 19b, approximately 91% of 5 μm MPs passed through outlets 2-5 while the rest were distributed across outlets 6-17. A total of 94% of the 11 μm MPs passed through outlets 6-9, while 82% of the 15 μm NMPs went through outlet 15. As 5μm MPs were found mixed with the streams of both 11 μm MPs and 15 μm NMPs, we calculated the sorting purity of both of these particles with respect to contamination of their streams by 5μm MPs. We found that 11 μm MPs were sorted from 5 μm MPs with a purity of 94%. The 15 μm NMPs were fractionated from 5 μm MPs with a purity of 98%. The streams of 5 μm and 11 μm MPs were found to be more dispersed compared to 15 μm NMPs as seen in Fig. 19a. This is potentially because of the 3D nature of magnetic forces acting on MPs which might have led to distribution of these particles across the height of the channel, while 15μm NMPs were mostly focused in the center of the channel due to elastic forces.

4.5 Conclusions

In summary, we demonstrated a sheathless mode of magnetophoretic sorting of three MPs and NMPs in non-Newtonian fluids with various viscosities. We anticipate that the sorting scheme is due to a combination of magnetic and elastic focusing of particles. Hypothetically, the MPs were pulled towards the wall of the channel and focused along it, while NMPs were focused in the center away from MPs because of elastic lift forces. The 5 μm and 11 μm MPs, focused along the wall, get separated from each other in expansion zone of the device in a PFF style. The parametric study conducted with respect to flow rate and PEO concentration aided in understanding the operating conditions needed for achieving separation. We found that increase in Weissenberg number, with increase in flow rate and PEO concentration, leads to focusing of

particles in multiple positions and interfere with sorting performance as the focusing of NMPs particles at the center of the channel is required for separation. This phenomenon must be further investigated and may become advantageous in performing sorting at high flow rates in non-Newtonian fluids. We envision the adoption of this technique in immunomagnetic separation of analytes like cells directly from sampled non-Newtonian fluids (e.g., blood) which can save a significant amount of time and resources in current sample preparation processes.

Chapter Five

5 Thesis Summary and Future Works

Here, we have summarized the major conclusions of this thesis. Also, we have provided a list of future works that could be pursued based on the knowledge gained from the undertaken research.

5.1 Thesis Summary

In this thesis, we presented a sorting technique for handling mixtures of MPs and NMPs in Newtonian and non-Newtonian fluid. Based on our literature review, we found that there were several technological gaps in the currently reported methods of sorting. The major drawbacks were requirement of a diluting sheath flow for running the device to achieve sorting, low throughput of sample processing, low separation purity, inability to perform multiplex sorting and complicated methods of fabricating magnetic elements into microfluidics devices. We have addressed the majority of these technological gaps using our proposed hybrid sorting technique in this thesis.

To achieve objective 1 of the thesis (outlined in chapter 1), we proposed the MHF technique, which has been devised by integrating the magnetic focusing with the concept of PFF. Essentially, we focused the MPs along the walls of a thin channel using magnetic field instead of any sheath flow, then achieved hydrodynamic fractionation in a style similar to PFF at a downstream expansion channel. This sheathless method of sorting does not need any complicated fabrication method and can be operated with a simple permanent magnet. Moreover, we found that the MHF technique is able to fractionate 5 μm and 11 μm MPs with an efficiency of 98% at a throughput of 10^7 particles per hour.

For objective 2 and 3, we proposed the MIMF technique by further combining the inertial focusing approach with MHF. We achieved duplex fractionation at a high throughput of 10^9 particles per hour. We found that under the combined effects of magnetic, inertial and drag forces, particles arrange themselves in the order of their sizes in the microchannel such that smaller particles stay closer to the wall of the channel. Utilizing this size based ordering, we fractionated four particles simultaneously and separated 5 μm, 11 μm and 35 μm MPs from 15 μm NMPs.

To achieve objective 4, we tested a viscoelastic fluid prepared by mixing PEO in water. We demonstrated separation of 5 μm and 11 μm MPs from 15 μm NMPs in fluids with various viscosities. The sorting was achieved in the MHF style, however we found that particles were significantly affected by elastic forces in the viscoelastic solutions. We performed experiments with respect to flow rate and PEO concentration, which helped us to determine the optimal operating conditions to achieve triplex fractionation and sorting in our device.

5.2 Future Studies

In this thesis, we provided an experimental study of sorting microparticles in Newtonian and non-Newtonian fluids in a novel microfluidic device. Based on the insights gained in this study, we propose further investigations to improve the understanding of underlying mechanism of separation and to demonstrate its application in sorting and separation of biological samples.

We believe it is important to develop numerical models to study the particles motion in the device using commercial tools such as COMSOL Multiphysics. Simulations would allow us to perform studies to investigate the effect of parameters, which we did not study in this thesis, such as length of magnet, width of channel and length of channel on fractionation performance in our device. Length of magnet should be optimized as the time for which particles are exposed to

magnetic field has a significant influence on exit position of particles in the device. Width of channel is another important factor and it needs to be optimized as it directly affects the magnitude of inertial forces acting on particles. The length of channel significantly influences the position of particles as longer length results in enhanced inertial and elastic focusing. We believe optimizing these parameters would aid in achieving even higher throughputs and fractionation purities. Simulation studies would also help in answering one of the major questions about quality of fractionation of particles in our device. It is important to determine how close the sizes of MPs can be to achieve separation in our device. Simulation studies could be a convenient tool to determine the effectiveness of our technique in fractionating closely sized MPs. It would also aid in modifying the design so that more than four particles could be sorted simultaneously.

Another important future work is to establish the applicability of this sorting technique to biological samples. We expect that two to four different microorganisms could be immunomagnetically attached to magnetic beads and sorted in our device based on the proposed MIMF or MHF sorting schemes in this thesis. These studies would demonstrate the usefulness of our device in handling biological samples, which further could be utilized for separating pathogens from water samples or isolating rare CTCs from blood.

Last but not least, it is important to study the effect of shape of particles on the sorting performance in our device experimentally as well as analytically. As cells would be attached to magnetic beads, the shape of cells and beads together would not be spherical and it might have an influence over the behavior of particles in the channel. It is desired that experiments be performed with particles having shapes such as ellipse, cocci and rod, as these are the most commonly found shapes of microorganisms.

Bibliography

[1] U. Schaflinger, Centrifugal separation of a mixture, Fluid Dyn. Res. 6 (1990) 213–249. doi:10.1016/0169-5983(90)90014-P.

[2] M.B. Dainiak, F.M. Plieva, I.Y. Galaev, R. Hatti-Kaul, B. Mattiasson, Cell Chromatography: Separation of Different Microbial Cells Using IMAC Supermacroporous Monolithic Columns, Biotechnol. Prog. 21 (2008) 644–649. doi:10.1021/bp049615g.

[3] M. Yamada, M. Seki, Hydrodynamic filtration for on-chip particle concentration and classification utilizing microfluidics., Lab Chip. 5 (2005) 1233–1239. doi:10.1039/b509386d.

[4] P. Gravesen, J. Branebjerg, O.S. Jensen, Microfluidics-a review, J. Micromechanics Microengineering. 3 (1993) 168–182. doi:10.1088/0960-1317/3/4/002.

[5] G.M. Whitesides, The origins and the future of microfluidics., Nature. 442 (2006) 368–373. doi:10.1038/nature05058.

[6] K. Ohno, K. Tachikawa, A. Manz, Microfluidics: Applications for analytical purposes in chemistry and biochemistry, Electrophoresis. 29 (2008) 4443–4453. doi:10.1002/elps.200800121.

[7] L. Sun, M. Zborowski, L.R. Moore, J.J. Chalmers, Continuous, flow-through immunomagnetic cell sorting in a quadrupole field, Cytometry. 33 (1998) 469–475. doi:10.1002/(SICI)1097-0320(19981201)33:4<469::AID-CYTO11>3.0.CO;2-6.

[8] S. Fiedler, S.G. Shirley, T. Schnelle, G. Fuhr, Dielectrophoretic Sorting of Particles and Cells in a Microsystem, Anal. Chem. 70 (1998) 1909–1915. doi:10.1021/ac971063b.

[9] M.P. MacDonald, G.C. Spalding, K. Dholakia, Microfluidic sorting in an optical lattice.,

Nature. 426 (2003) 421–4. doi:10.1038/nature02144.

[10] F. Petersson, A. Lena, A. Swa, T. Laurell, Free Flow Acoustophoresis : Microfluidic-Based Mode of Particle and Cell Separation, Anal. Chem. 79 (2007) 5117–5123.

[11] M. Yamada, M. Nakashima, M. Seki, Pinched flow fractionation: Continuous size separation of particles utilizing a laminar flow profile in a pinched microchannel, Anal. Chem. 76 (2004) 5465–5471. doi:10.1021/ac049863r.

[12] D. Di Carlo, D. Irimia, R.G. Tompkins, M. Toner, Continuous inertial focusing, ordering, and separation of particles in microchannels., Proc. Natl. Acad. Sci. U. S. A. 104 (2007) 18892–7. doi:10.1073/pnas.0704958104.

[13] L.R. Huang, E.C. Cox, R.H. Austin, J.C. Sturm, Continuous particle separation through deterministic lateral displacement., Science. 304 (2004) 987–990. doi:10.1126/science.1094567.

[14] N. Pamme, A. Manz, On-chip free-flow magnetophoresis: Continuous flow separation of magnetic particles and agglomerates, Anal. Chem. 76 (2004) 7250–7256. doi:10.1021/ac049183o.

[15] R. Rong, J.-W. Choi, C.H. Ahn, An on-chip magnetic bead separator for biocell sorting, J. Micromechanics Microengineering. 16 (2006) 2783–2790. doi:10.1088/0960-1317/16/12/035.

[16] M. Zborowski, J.J. Chalmers, Rare Cell Separation and Analysis by Magnetic Sorting, Anal. Chem. 83 (2011) 8050–8056. doi:10.1021/ac200550d.

[17] Q. Ramadan, L. Christophe, W. Teo, L. ShuJun, F.H. Hua, Flow-through immunomagnetic separation system for waterborne pathogen isolation and detection: Application to Giardia and Cryptosporidium cell isolation, Anal. Chim. Acta. 673 (2010)

101–108. doi:10.1016/j.aca.2010.05.025.

[18] J.D. Adams, U. Kim, H.T. Soh, Multitarget magnetic activated cell sorter., Proc. Natl. Acad. Sci. U. S. A. 105 (2008) 18165–18170. doi:10.1073/pnas.0809795105.

[19] J. Chalmers, M. Zborowski, Flow through, immunomagnetic cell separation, Biotechnol. …. (1998). http://onlinelibrary.wiley.com/doi/10.1021/bp970140l/full (accessed December 14, 2015).

[20] † Jason G. Kralj, † Michael T. W. Lis, ‡ and Martin A. Schmidt, † Klavs F. Jensen*, Continuous Dielectrophoretic Size-Based Particle Sorting, (2006). doi:10.1021/AC0601314.

[21] L. Ren, Y. Chen, P. Li, Z. Mao, P.-H. Huang, J. Rufo, F. Guo, L. Wang, J.P. McCoy, S.J. Levine, T.J. Huang, A high-throughput acoustic cell sorter, Lab Chip. 15 (2015) 3870–3879. doi:10.1039/C5LC00706B.

[22] S. Yan, J. Zhang, M. Li, G. Alici, H. Du, R. Sluyter, W. Li, On-chip high-throughput manipulation of particles in a dielectrophoresis-active hydrophoretic focuser, Sci. Rep. 4 (2014) 1–8. doi:10.1038/srep05060.

[23] X. Xuan, J. Zhu, C. Church, Particle focusing in microfluidic devices, Microfluid. Nanofluidics. 9 (2010) 1–16. doi:10.1007/s10404-010-0602-7.

[24] P.R.C. Gascoyne, X.B. Wang, Y. Huang, R.F. Becker, Dielectrophoretic separation of cancer cells from blood, IEEE Trans. Ind. Appl. 33 (1997) 670–678. doi:10.1109/28.585856.

[25] U. Kim, H.T. Soh, Simultaneous sorting of multiple bacterial targets using integrated dielectrophoretic-magnetic activated cell sorter., Lab Chip. 9 (2009) 2313–2318. doi:10.1039/b903950c.

[26] P. Li, Z. Mao, Z. Peng, L. Zhou, Y. Chen, P.-H. Huang, C.I. Truica, J.J. Drabick, W.S. El-Deiry, M. Dao, S. Suresh, T.J. Huang, Acoustic separation of circulating tumor cells., Proc. Natl. Acad. Sci. U. S. A. 112 (2015) 4970–4975. doi:10.1073/pnas.1504484112.

[27] A.H.J. Yang, H.T. Soh, Acoustophoretic Sorting of Viable Mammalian Cells in a Microfluidic Device, Anal. Chem. 84 (2012) 10756–10762. doi:10.1021/ac3026674.

[28] M.M. Wang, E. Tu, D.E. Raymond, J.M. Yang, H. Zhang, N. Hagen, B. Dees, E.M. Mercer, A.H. Forster, I. Kariv, P.J. Marchand, W.F. Butler, Microfluidic sorting of mammalian cells by optical force switching., Nat. Biotechnol. 23 (2005) 83–87. doi:10.1038/nbt1050.

[29] B. Landenberger, H. Hofemann, S. Wadle, A. Rohrbach, Microfluidic sorting of arbitrary cells with dynamic optical tweezers, Lab Chip. 12 (2012) 3177–3183. doi:10.1039/C2LC21099A.

[30] X. Wang, S. Chen, M. Kong, Z. Wang, K.D. Costa, R.A. Li, D. Sun, Enhanced cell sorting and manipulation with combined optical tweezer and microfluidic chip technologies, Lab Chip. 11 (2011) 3656. doi:10.1039/c1lc20653b.

[31] M. Pødenphant, N. Ashley, K. Koprowska, K.U. Mir, M. Zalkovskij, B. Bilenberg, W. Bodmer, A. Kristensen, R. Marie, Separation of cancer cells from white blood cells by pinched flow fractionation, Lab Chip. 15 (2015) 4598–4606. doi:10.1039/C5LC01014D.

[32] A.V. Larsen, L. Poulsen, H. Birgens, M. Dufva, A. Kristensen, Pinched flow fractionation devices for detection of single nucleotide polymorphisms., Lab Chip. 8 (2008) 818–821. doi:10.1039/b802268b.

[33] † Hirosuke Maenaka, ‡ Masumi Yamada, † and Masahiro Yasuda, †,§ Minoru Seki*, Continuous and Size-Dependent Sorting of Emulsion Droplets Using Hydrodynamics in

Pinched Microchannels, (2008). doi:10.1021/LA703581J.

[34] M.P. Kok, T. Segers, M. Versluis, Bubble sorting in pinched microchannels for ultrasound contrast agent enrichment, Lab Chip. 15 (2015) 3716–3722. doi:10.1039/C5LC00370A.

[35] J. Takagi, M. Yamada, M. Yasuda, M. Seki, Continuous particle separation in a microchannel having asymmetrically arranged multiple branches., Lab Chip. 5 (2005) 778–784. doi:10.1039/b501885d.

[36] C. Jin, S.M. McFaul, S.P. Duffy, X. Deng, P. Tavassoli, P.C. Black, H. Ma, Technologies for label-free separation of circulating tumor cells: from historical foundations to recent developments, Lab Chip. 14 (2014) 32–44. doi:10.1039/C3LC50625H.

[37] M. Yamada, M. Seki, Hydrodynamic filtration for on-chip particle concentration and classification utilizing microfluidics, Lab Chip. 5 (2005) 1233. doi:10.1039/b509386d.

[38] J. Zhou, P.V. Giridhar, S. Kasper, I. Papautsky, Modulation of aspect ratio for complete separation in an inertial microfluidic channel3, 13 (2013). doi:10.1039/c3lc50101a.

[39] S.S. Kuntaegowdanahalli, A.A.S. Bhagat, G. Kumar, I. Papautsky, Inertial microfluidics for continuous particle separation in spiral microchannels, Lab Chip. 9 (2009) 2973. doi:10.1039/b908271a.

[40] Z. Liu, F. Huang, J. Du, W. Shu, H. Feng, X. Xu, Y. Chen, Rapid isolation of cancer cells using microfluidic deterministic lateral displacement structure, Biomicrofluidics. 7 (2013) 11801. doi:10.1063/1.4774308.

[41] S.H. Holm, J.P. Beech, M.P. Barrett, J.O. Tegenfeldt, Separation of parasites from human blood using deterministic lateral displacement, Lab Chip. 11 (2011) 1326. doi:10.1039/c0lc00560f.

[42] J. McGrath, M. Jimenez, H. Bridle, Deterministic lateral displacement for particle

separation: a review., Lab Chip. 14 (2014) 4139–58. doi:10.1039/c4lc00939h.

[43] M. Mizuno, M. Yamada, R. Mitamura, K. Ike, K. Toyama, M. Seki, Magnetophoresis-integrated hydrodynamic filtration system for size-and surface marker-based two-dimensional cell sorting, Anal. Chem. 85 (2013) 7666–7673. doi:10.1021/ac303336f.

[44] M.G. Lee, J.H. Shin, C.Y. Bae, S. Choi, J.-K. Park, Label-free cancer cell separation from human whole blood using inertial microfluidics at low shear stress., Anal. Chem. 85 (2013) 6213–8. doi:10.1021/ac4006149.

[45] J.M. Martel, M. Toner, Inertial focusing in microfluidics., Annu. Rev. Biomed. Eng. 16 (2014) 371–96. doi:10.1146/annurev-bioeng-121813-120704.

[46] D. Di Carlo, Inertial microfluidics, Lab Chip. 9 (2009) 3038. doi:10.1039/b912547g.

[47] M.E. Warkiani, G. Guan, K.B. Luan, W.C. Lee, A.A.S. Bhagat, P.K. Chaudhuri, D.S.-W. Tan, W.T. Lim, S.C. Lee, P.C.Y. Chen, C.T. Lim, J. Han, Slanted spiral microfluidics for the ultra-fast, label-free isolation of circulating tumor cells., Lab Chip. 14 (2014) 128–37. doi:10.1039/c3lc50617g.

[48] A. Sarkar, H.W. Hou, A.E. Mahan, J. Han, G. Alter, Multiplexed Affinity-Based Separation of Proteins and Cells Using Inertial Microfluidics., Sci. Rep. 6 (2016) 23589. doi:10.1038/srep23589.

[49] J. Chen, J. Li, Y. Sun, Microfluidic approaches for cancer cell detection, characterization, and separation., Lab Chip. 12 (2012) 1753–67. doi:10.1039/c2lc21273k.

[50] S. Nagrath, L. V Sequist, S. Maheswaran, D.W. Bell, D. Irimia, L. Ulkus, M.R. Smith, E.L. Kwak, S. Digumarthy, A. Muzikansky, P. Ryan, U.J. Balis, R.G. Tompkins, D.A. Haber, M. Toner, Isolation of rare circulating tumour cells in cancer patients by microchip technology., Nature. 450 (2007) 1235–9. doi:10.1038/nature06385.

[51] S.D. Richardson, T.A. Ternes, Water analysis: emerging contaminants and current issues., Anal. Chem. 86 (2014) 2813–48. doi:10.1021/ac500508t.

[52] O. Rotariu, I.D. Ogden, M. MacRae, V. Bădescu, N.J.C. Strachan, An immunomagnetic separator for concentration of pathogenic micro-organisms from large volume samples, J. Magn. Magn. Mater. 293 (2005) 589–596. doi:10.1016/j.jmmm.2005.01.078.

[53] A.H.C. Ng, U. Uddayasankar, A.R. Wheeler, Immunoassays in microfluidic systems, Anal. Bioanal. Chem. 397 (2010) 991–1007. doi:10.1007/s00216-010-3678-8.

[54] M.C. Bélanger, Y. Marois, Hemocompatibility, biocompatibility, inflammatory and in vivo studies of primary reference materials low-density polyethylene and polydimethylsiloxane: A review, J. Biomed. Mater. Res. 58 (2001) 467–477. doi:10.1002/jbm.1043.

[55] C.A. Baker, C.T. Duong, A. Grimley, M.G. Roper, Recent advances in microfluidic detection systems., Bioanalysis. 1 (2009) 967–75. doi:10.4155/bio.09.86.

[56] A.M. Streets, Y. Huang, Chip in a lab : Microfluidics for next generation life science research Chip in a lab : Microfluidics for next generation life science, 11302 (2013) 1–23. doi:10.1063/1.4789751.

[57] R.W. Applegate, J. Squier, T. Vestad, J. Oakey, D.W.M. Marr, P. Bado, M. a Dugan, A. a Said, Microfluidic sorting system based on optical waveguide integration and diode laser bar trapping., Lab Chip. 6 (2006) 422–426. doi:10.1039/b512576f.

[58] A. Valero, T. Braschler, N. Demierre, P. Renaud, A miniaturized continuous dielectrophoretic cell sorter and its applications, Biomicrofluidics. 4 (2010) 1–9. doi:10.1063/1.3430542.

[59] L.R. Huang, E.C. Cox, R.H. Austin, J.C. Sturm, Continuous Particle Separation Through

Deterministic Lateral Displacement, Science (80-.). 304 (2004) 987–990.

[60] H. Mohamed, J.N. Turner, M. Caggana, Biochip for separating fetal cells from maternal circulation, J. Chromatogr. A. 1162 (2007) 187–192. doi:10.1016/j.chroma.2007.06.025.

[61] P. Sajeesh, A.K. Sen, Particle separation and sorting in microfluidic devices: a review, Microfluid. Nanofluidics. 17 (2013) 1–52. doi:10.1007/s10404-013-1291-9.

[62] C.W. Shields, C.D. Reyes, G.P. López, Microfluidic cell sorting: a review of the advances in the separation of cells from debulking to rare cell isolation., Lab Chip. 15 (2015) 1230–49. doi:10.1039/c4lc01246a.

[63] O.O. Saeed, R. Li, Y. Deng, Microfluidic Approaches for Cancer Cell Separation: Review, J. Biomed. Sci. Eng. 7 (2014) 1005–1018. doi:10.4236/jbise.2014.712098.

[64] Y. Sai, M. Yamada, M. Yasuda, M. Seki, Continuous separation of particles using a microfluidic device equipped with flow rate control valves, J. Chromatogr. A. 1127 (2006) 214–220. doi:10.1016/j.chroma.2006.05.020.

[65] M. Moini, Design and Performance of a Universal Sheathless Capillary Electrophoresis to Mass Spectrometry Interface Using a Split-Flow Technique, Anal. Chem. 73 (2001) 3497–3501. doi:10.1021/ac010189c.

[66] M. Matsuda, M. Yamada, M. Seki, Blood cell classification utilizing hydrodynamic filtration, Electron. Commun. Japan. 94 (2011) 1–6. doi:10.1002/ecj.10281.

[67] H.M. Ji, V. Samper, Y. Chen, C.K. Heng, T.M. Lim, L. Yobas, Silicon-based microfilters for whole blood cell separation, Biomed. Microdevices. 10 (2008) 251–257. doi:10.1007/s10544-007-9131-x.

[68] A.-L. Gassner, M. Abonnenc, H.-X. Chen, J. Morandini, J. Josserand, J.S. Rossier, J.-M. Busnel, H.H. Girault, Magnetic forces produced by rectangular permanent magnets in

static microsystems., Lab Chip. 9 (2009) 2356–63. doi:10.1039/b901865d.

[69] C. Hoffmann, M. Franzreb, W.H. Höll, A novel high-gradient magnetic separator (HGMS) design for biotech applications, IEEE Trans. Appl. Supercond. 12 (2002) 963–966. doi:10.1109/TASC.2002.1018560.

[70] N. Xia, T.P. Hunt, B.T. Mayers, E. Alsberg, G.M. Whitesides, R.M. Westervelt, D.E. Ingber, Combined microfluidic-micromagnetic separation of living cells in continuous flow, Biomed. Microdevices. 8 (2006) 299–308. doi:10.1007/s10544-006-0033-0.

[71] S.S. Shevkoplyas, A.C. Siegel, R.M. Westervelt, M.G. Prentiss, G.M. Whitesides, The force acting on a superparamagnetic bead due to an applied magnetic field., Lab Chip. 7 (2007) 1294–1302. doi:10.1039/b705045c.

[72] J.C. McDonald, G.M. Whitesides, Poly(dimethylsiloxane) as a material for fabricating microfluidic devices, Acc. Chem. Res. 35 (2002) 491–499. doi:10.1021/ar010110q.

[73] O. Shardt, S.K. Mitra, J.J. Derksen, Lattice Boltzmann simulations of pinched flow fractionation, Chem. Eng. Sci. 75 (2012) 106–119. doi:10.1016/j.ces.2012.03.013.

[74] J. Zhou, I. Papautsky, Fundamentals of inertial focusing in microchannels., Lab Chip. 13 (2013) 1121–32. doi:10.1039/c2lc41248a.

[75] A.J. Mach, D. Di Carlo, Continuous scalable blood filtration device using inertial microfluidics., Biotechnol. Bioeng. 107 (2010) 302–11. doi:10.1002/bit.22833.

[76] A.A.S. Bhagat, S.S. Kuntaegowdanahalli, I. Papautsky, Enhanced particle filtration in straight microchannels using shear-modulated inertial migration, Phys. Fluids. 20 (2008) 1–4. doi:10.1063/1.2998844.

[77] D. Di Carlo, D. Irimia, R.G. Tompkins, M. Toner, Continuous inertial focusing, ordering, and separation of particles in microchannels., Proc. Natl. Acad. Sci. U. S. A. 104 (2007)

18892–7. doi:10.1073/pnas.0704958104.

[78] H. Andersson, A. van den Berg, Microfluidic devices for cellomics: a review, Sensors Actuators B Chem. 92 (2003) 315–325. doi:10.1016/S0925-4005(03)00266-1.

[79] S. Yilmaz, A.K. Singh, Single cell genome sequencing., Curr. Opin. Biotechnol. 23 (2012) 437–43. doi:10.1016/j.copbio.2011.11.018.

[80] A.-E. Saliba, L. Saias, E. Psychari, N. Minc, D. Simon, F.-C. Bidard, C. Mathiot, J.-Y. Pierga, V. Fraisier, J. Salamero, V. Saada, F. Farace, P. Vielh, L. Malaquin, J.-L. Viovy, Microfluidic sorting and multimodal typing of cancer cells in self-assembled magnetic arrays., Proc. Natl. Acad. Sci. U. S. A. 107 (2010) 14524–9. doi:10.1073/pnas.1001515107.

[81] E. Ozkumur, A.M. Shah, J.C. Ciciliano, B.L. Emmink, T. David, E. Brachtel, M. Yu, P. Chen, B. Morgan, J. Trautwein, A. Kimura, S. Sengupta, S.L. Stott, N.M. Karabacak, T. a Barber, J.R. Walsh, K. Smith, P.S. Spuhler, J.P. Sullivan, R.J. Lee, D.T. Ting, X. Luo, A.T. Shaw, A. Bardia, V. Lecia, D.N. Louis, S. Maheswaran, R. Kapur, D. a Haber, Inertial Focusing for Tumor Antigen–Dependent and – Independent Sorting of Rare Circulating Tumor Cells, Sci Transl Med. 5 (2013) 1–20. doi:10.1126/scitranslmed.3005616.Inertial.

[82] C.T. Lim, Y. Zhang, Bead-based microfluidic immunoassays: the next generation., Biosens. Bioelectron. 22 (2007) 1197–204. doi:10.1016/j.bios.2006.06.005.

[83] M.H. Julius, T. Masuda, L.A. Herzenberg, Demonstration that antigen-binding cells are precursors of antibody-producing cells after purification with a fluorescence-activated cell sorter., Proc. Natl. Acad. Sci. U. S. A. 69 (1972) 1934–8. http://www.pubmedcentral.nih.gov/articlerender.fcgi?artid=426835&tool=pmcentrez&ren

dertype=abstract (accessed October 17, 2015).

[84] A.A.S. Bhagat, S.S. Kuntaegowdanahalli, N. Kaval, C.J. Seliskar, I. Papautsky, Inertial microfluidics for sheath-less high-throughput flow cytometry, Biomed. Microdevices. 12 (2010) 187–195. doi:10.1007/s10544-009-9374-9.

[85] A. Sarkar, H.W. Hou, A.E. Mahan, J. Han, G. Alter, Multiplexed Affinity-Based Separation of Proteins and Cells Using Inertial Microfluidics., Sci. Rep. 6 (2016) 23589. doi:10.1038/srep23589.

[86] G.-P. Zhu, M. Hejiazan, X. Huang, N.-T. Nguyen, Magnetophoresis of diamagnetic microparticles in a weak magnetic field, Lab Chip. 14 (2014) 4609–4615. doi:10.1039/C4LC00885E.

[87] S. Miltenyi, W. Muller, W. Weichel, A. Radbruch, High Gradient Magnetic Cell Separation With MACS, Cytometry. 11 (1990) 231–238. doi:10.1002/cyto.990110203.

[88] D.W. Inglis, R. Riehn, R.H. Austin, J.C. Sturm, Continuous microfluidic immunomagnetic cell separation, Appl. Phys. Lett. 85 (2004) 5093–5095. doi:10.1063/1.1823015.

[89] J. Oberteuffer, High gradient magnetic separation, IEEE Trans. Magn. 12 (2002) 967–970.

[90] F. Del Giudice, H. Madadi, M.M. Villone, G. D'Avino, A.M. Cusano, R. Vecchione, M. Ventre, P.L. Maffettone, P. a. Netti, Magnetophoresis "meets" viscoelasticity: deterministic separation of magnetic particles in a modular microfluidic device, Lab Chip. 15 (2015) 1912–1922. doi:10.1039/C5LC00106D.

[91] S.S.H. Tsai, I.M. Griffiths, H. a Stone, Microfluidic immunomagnetic multi-target sorting--a model for controlling deflection of paramagnetic beads., Lab Chip. 11 (2011) 2577–2582. doi:10.1039/c1lc20153k.

[92] V. Kumar, P. Rezai, Sheathless and High Throughput Sorting of Paramagnetic Microparticles in a Magneto-Hydrodynamic Microfluidic Device, IEEE EMBC 2016, Orlando FL, USA, In Press, IEEE EMBC. In Press (2016).

[93] J.J. Chalmers, M. Zborowski, L. Sun, L. Moore, Flow through, immunomagnetic cell separation, Biotechnol. Prog. 14 (1998) 141–148. doi:10.1021/bp970140l.

[94] X. Wang, C. Liedert, R. Liedert, I. Papautsky, A disposable, roll-to-roll hot-embossed inertial microfluidic device for size-based sorting of microbeads and cells, Lab Chip. 16 (2016) 1821–1830. doi:10.1039/C6LC00215C.

[95] C. Liu, G. Hu, X. Jiang, J. Sun, Inertial focusing of spherical particles in rectangular microchannels over a wide range of Reynolds numbers, Lab Chip. 15 (2015) 1168–1177. doi:10.1039/C4LC01216J.

[96] Z. Wu, Y. Chen, M. Wang, A.J. Chung, Continuous inertial microparticle and blood cell separation in straight channels with local microstructures, Lab Chip. 16 (2016) 532–542. doi:10.1039/C5LC01435B.

[97] G. SEGRÉ, A. SILBERBERG, Radial Particle Displacements in Poiseuille Flow of Suspensions, Nature. 189 (1961) 209–210. doi:10.1038/189209a0.

[98] D. Mattanovich, N. Borth, Applications of cell sorting in biotechnology, Microb. Cell Fact. 5 (2006) 12. doi:10.1186/1475-2859-5-12.

[99] C. Rivet, H. Lee, A. Hirsch, S. Hamilton, H. Lu, Microfluidics for medical diagnostics and biosensors, Chem. Eng. Sci. 66 (2011) 1490–1507. doi:10.1016/j.ces.2010.08.015.

[100] S. Kim, S.-I. Han, M.-J. Park, C.-W. Jeon, Y.-D. Joo, I.-H. Choi, K.-H. Han, Circulating Tumor Cell Microseparator Based on Lateral Magnetophoresis and Immunomagnetic Nanobeads, Anal. Chem. 85 (2013) 2779–2786. doi:10.1021/ac303284u.

[101] * Stefan Fiedler, Stephen G. Shirley, and Thomas Schnelle, G. Fuhr, Dielectrophoretic Sorting of Particles and Cells in a Microsystem, (1998). doi:10.1021/AC971063B.

[102] L. Schmid, D.A. Weitz, T. Franke, Sorting drops and cells with acoustics: acoustic microfluidic fluorescence-activated cell sorter, Lab Chip. 14 (2014) 3710. doi:10.1039/C4LC00588K.

[103] Siyang Zheng, Raylene Yung, Yu-Chong Tai, H. Kasdan, Determinstic lateral displacement mems device for continuous blood cell separation, in: 18th IEEE Int. Conf. Micro Electro Mech. Syst. 2005. MEMS 2005., IEEE, n.d.: pp. 851–854. doi:10.1109/MEMSYS.2005.1454063.

[104] M. Nakashima, M. Yamada, M. Seki, Pinched flow fractionation (PFF) for continuous particle separation in a microfluidic device, in: 17th IEEE Int. Conf. Micro Electro Mech. Syst. Maastricht MEMS 2004 Tech. Dig., IEEE, n.d.: pp. 33–36. doi:10.1109/MEMS.2004.1290515.

[105] H.A. Nieuwstadt, R. Seda, D.S. Li, J.B. Fowlkes, J.L. Bull, Microfluidic particle sorting utilizing inertial lift force, Biomed. Microdevices. 13 (2011) 97–105. doi:10.1007/s10544-010-9474-6.

[106] J.D. Adams, P. Thévoz, H. Bruus, H.T. Soh, Integrated acoustic and magnetic separation in microfluidic channels, Appl. Phys. Lett. 95 (2009) 254103. doi:10.1063/1.3275577.

[107] C. V Mura, M.I. Becker, A. Orellana, D. Wolff, Immunopurification of Golgi vesicles by magnetic sorting, J. Immunol. Methods. 260 (2002) 263–271. doi:10.1016/S0022-1759(01)00546-4.

[108] Z. Jiang, J. Llandro, T. Mitrelias, J.A.C. Bland, An integrated microfluidic cell for detection, manipulation, and sorting of single micron-sized magnetic beads, J. Appl. Phys.

99 (2006) 08S105. doi:10.1063/1.2176238.

[109] N.S. and, †,‡ Mark A. Burns*, Analysis of Non-Newtonian Liquids Using a Microfluidic Capillary Viscometer, (2006).

[110] F.J.H. Gijsen, F.N. van de Vosse, J.D. Janssen, The influence of the non-Newtonian properties of blood on the flow in large arteries: steady flow in a carotid bifurcation model, J. Biomech. 32 (1999) 601–608. doi:10.1016/S0021-9290(99)00015-9.

[111] F. Del Giudice, G. Romeo, G. D'Avino, F. Greco, P.A. Netti, P.L. Maffettone, Particle alignment in a viscoelastic liquid flowing in a square-shaped microchannel., Lab Chip. 13 (2013) 4263–71. doi:10.1039/c3lc50679g.

[112] X. Lu, L. Zhu, R. mao Hua, X. Xuan, Continuous sheath-free separation of particles by shape in viscoelastic fluids, Appl. Phys. Lett. 107 (2015) 18–23. doi:10.1063/1.4939267.

[113] S. Yang, J.Y. Kim, S.J. Lee, S.S. Lee, J.M. Kim, Sheathless elasto-inertial particle focusing and continuous separation in a straight rectangular microchannel, Lab Chip. 11 (2011) 266–273. doi:10.1039/C0LC00102C.

[114] C. Liu, C. Xue, X. Chen, L. Shan, Y. Tian, G. Hu, Size-Based Separation of Particles and Cells Utilizing Viscoelastic Effects in Straight Microchannels, Anal. Chem. 87 (2015) 6041–6048. doi:10.1021/acs.analchem.5b00516.